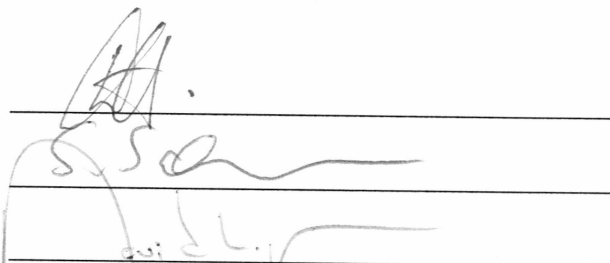


MEASUREMENT OF EFFECTIVE DIFFUSION ON ANDESITE ROCK,  
AMCHITKA ISLAND, ALASKA.

By

Srinivas Rao Raghupatruni

RECOMMENDED:


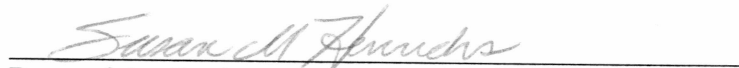
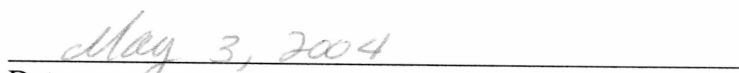


Advisory Committee Chair



Chair, Department of Civil and Environmental  
Engineering

APPROVED:

  
Dean, College of Science, Engineering and Mathematics  
Dean of the Graduate School  
Date

**MEASUREMENT OF EFFECTIVE DIFFUSION ON  
ANDESITE ROCK, AMCHITKA ISLAND, ALASKA.**

A  
THESIS

Presented to the Faculty  
of the University of Alaska Fairbanks

In Partial Fulfillment of the Requirements  
for the Degree of

MASTER OF SCIENCE

By

Srinivas Rao Raghupatruni

Fairbanks, Alaska

May 2004

ALASKA  
TD  
427  
R3  
R34  
2004



## ABSTRACT

Between 1965 and 1971 three nuclear weapon tests were conducted on Amchitka Island, Alaska. Currently research is being conducted to understand the possible movement of radionuclides through the Island subsurface into the marine environment so that a monitoring system can be developed. The possibility of radionuclide diffusion into matrix rock surrounding fracture pathways needs to be better understood. This thesis presents ongoing research with the goal of determining the effective diffusion coefficients for andesite rock found in the Island subsurface. These studies are being conducted in a bench scale reactor consisting of two chambers separated by a sliced rock core obtained from the Island. The increase in conservative tracer over time is measured in the receiving chamber. The effective diffusion coefficients are then determined by applying these results to a solution to Fick's Second Law. Results from these studies will be used in the development of a long term monitoring program for the island.

## TABLE OF CONTENTS

SIGNATURE PAGE	i
TITLE PAGE	ii
ABSTRACT	iii
TABLE OF CONTENTS	iv
LIST OF FIGURES	vii
LIST OF TABLES	iix
LIST OF APPENDICES	x
ACKNOWLEDGEMENT	xi

### **CHAPTER 1 INTRODUCTION** 1

Hypothesis	3
------------	---

### **CHAPTER 2 LITERATURE REVIEW** 4

2.1 Amchitka Island	4
---------------------	---

2.2 Topography	6
----------------	---

2.3 Geological history	6
------------------------	---

2.4 Weather and Climate	8
-------------------------	---

2.5 Tests Conducted on Amchitka Island	8
--	---

2.6 Diffusion	10
<b>CHAPTER 3 METHODOLOGY</b>	<b>21</b>
3.1 Leuco Crystal Violet Method	21
3.2 Through Diffusion	22
3.3 Elution Test	25
3.4 Porosity Measurements	25
3.5 Control Tests	26
<b>CHAPTER 4 RESULTS</b>	<b>28</b>
4.1 Sample 1 Through Diffusion Test	28
4.2 Sample 2 Through Diffusion Test	30
4.3 Sample 1 Elution Test	31
4.4 Sample 2 Elution Test	32
4.5 Porosity	34
4.6 Control Tests	35
<b>CHAPTER 5 DISCUSSION</b>	<b>36</b>
5.1 Numerical Estimation of Effective Diffusion Coefficients	36
5.2 Sample 2 Through Diffusion Test	39

5.3 Sample 2 Elution Test	43
5.4 Sample 1 Elution Test	47
5.5 Spacial Dependency of Effective Diffusion Coefficient	50
<b>CHAPTER 6 CONCLUSION</b>	<b>53</b>
Recommendations for future research	55
REFERENCES	<b>56</b>

## LIST OF FIGURES

Figure 2.1. Amchitka Island position.....	5
Figure 2.2. Map of Amchitka Island, Alaska- showing three nuclear detonation test sites	5
Figure 4.1. Concentration of iodide as a function of time in the source and receiving cells obtained from a through diffusion test on rock sample 1.....	29
Figure 4.2. Concentration of iodide as a function of time in the source and receiving cells obtained from a through diffusion test on rock sample 2.....	30
Figure 4.3. Concentration of iodide as a function of time obtained from an elution test on rock sample 1.....	32
Figure 4.4. Concentration of iodide as a function of time obtained from an elution test on rock sample 2.....	33
Figure 5.1. Finite element grid and boundary and initial conditions for the numerical solution to the Fick's Second Law applied to the through diffusion test.....	37
Figure 5.2. Finite element grid and boundary and initial conditions for the numerical solution to the Fick's Second Law applied to the elution test.....	39
Figure 5.3. Best fit of numerical model results to source cell experimental data for the through diffusion test on sample 2.....	40
Figure 5.4. Best fit of numerical model results to receiving cell experimental data for the through diffusion test on sample 2.....	41
Figure 5.5. Comparison of numerical model results to elution test for sample 2.....	44
Figure 5.6. Comparison of numerical model to elution test of sample 2 for various $D_e$ values.....	46

Figure 5.7. Comparison of numerical model results to elution test for sample 1 .....	47
Figure 5.8. Comparison of numerical model to elution test of sample 1 for various $D_e$ values. ....	48
Figure.5.9. Picture of rock sample 2 .....	51
Figure 5.10.Drying of the rock from (a) to (d) .....	51
Figure A.1. Calibration curve for first through diffusion test.....	60
Figure A.2. Calibration curve for second through diffusion test. ....	62

## LIST OF TABLES

Table 2.1. Reported values of Effective Diffusion Coefficients ( $D_e$ ). _____	19
Table 2.2. Reported values of Porosities _____	20
Table 4.1. Porosity measurements of two rock samples _____	35
Table 5.1. Mean square error for Sample 2 for various $D_e$ values _____	45
Table 5.2. Mean square error for Sample 1 for various $D_e$ values _____	49
Table 5.3. Effective diffusion coefficients of Andesite rock _____	49
Table A.1. Experimental data for Through Diffusion test 1 _____	60
Table A.2. Experimental data for elution test 1 _____	62
Table A.3. Experimental data for Through Diffusion test 2 _____	63
Table A.4. Experimental data for elution test 2 _____	64

## LIST OF APPENDICES

APPENDIX A	EXPERIMENTAL DATA	60
APPENDIX B	MODEL PROGRAM	65



## ACKNOWLEDGEMENT

Water and Environmental Research funded the second part of my research and the first part was funded by Department of Energy, CRESP organization.

I am indebted to Dr. David L. Barnes who as a faculty advisor supervised the research, providing ideas, suggestions and encouragement when problems arose and in completion of this thesis.

I would like to express my profound gratitude to my other committee members Dr. Dan White and Dr. Silke Schiewer for their guidance, valuable suggestions and their time during the course of the project.

I would also like to express my deepest thanks to Quinton Costello who ensured utmost precautions and safety measurements during conducting the lab work, Jennifer Benning for helping me in the lab work and my research team for their support.

My parents have been a source of support and encouragement through out the years, without whom I would have ever made up to this point. Last but not the least I would like to appreciate my brother and friends for their support and encouragement.

## **CHAPTER 1**

### **INTRODUCTION**

During the Cold War the United States government conducted extensive nuclear weapons testing at various sites, which in turn resulted in the contamination of surface and subsurface soils and water. These detonations led to the release of many hazardous minerals like radioactive materials Cs-137, St-90, and toxic metals such as lead. These hazardous materials cause a serious threat to human and environmental health. To protect human and the environmental health it was important to understand the movement of contaminants through the environments.

The majority of the underground nuclear testing conducted in the United States occurred at the Nevada Test Site (NTS) near Las Vegas, Nevada. The close proximity of NTS to Las Vegas limited the size of weapon that could safely be tested. Amchitka Island, Alaska was chosen as the site to test the weapons not suitable for NTS.

The mechanisms that control the movement of radionuclides and other contaminants through the NTS subsurface are fundamentally different than the mechanisms that control the movement of these compounds through the Amchitka Island subsurface. The NTS subsurface consists mainly of unconsolidated porous media. However, the Amchitka Island subsurface is fractured and faulted volcanic rock. Complexity is added to the fate and transport of contaminants when the subsurface

medium is consolidated rock and the primary groundwater flow pathways are through fractures in the media. Transport of radionuclides in groundwater flowing through fractures may result in diffusion of the contaminants into the surrounding rock, sometimes referred to as matrix rock. In these systems, diffusion will continue into the matrix rock until concentrations in the groundwater flowing through the fractures decreases to a level that will allow the radionuclides to diffuse from the matrix rock back into the fractures, thus remobilizing the contaminants.

The long term stewardship of Amchitka Island requires a monitoring program. Currently, only surface water on the Island is being periodically sampled. However, the gradient of the flow of groundwater that may contain radionuclides produced during the testing of nuclear devices is not towards surface water but to the ocean surrounding Amchitka. Thus, monitoring of the surface water on Amchitka provides no indication as to whether radionuclides are moving into an environment that may pose a risk to human and environmental health. A logical alternative to monitoring surface water on Amchitka is to monitor the marine environment surrounding the test locations on Amchitka.

Knowledge of the diffusive flux rate is essential to the prediction of the mass flux rate of radionuclides from the subsurface into the marine environment. Amchitka Island is a very unique and remote contaminated site. A successful monitoring program for this Island requires the ability to plan far in advance of sampling events.

Understanding the mass flux rate of radionuclides will provide planners with the ability to decide when sampling should occur. For example if the mass flux rate is relatively slow, then sampling events may be less frequent as opposed to the frequency if the flux rate is relatively fast. One of the key parameters that were required for a monitoring program to be developed was the effective diffusion coefficient that controls the diffusion flux rate from the fractures into the surround matrix rock. The purpose of this project is to measure the effective diffusion coefficient for a rock sample obtained from the Island's subsurface that is representative of a typical classification of rock found on Amchitka.

## **Hypothesis**

Diffusion will influence the movement of radionuclides through the subsurface andesite rocks found on Amchitka Island.

To test this hypothesis, laboratory through diffusion tests and elution tests were performed on slices of andesite core obtained from Amchitka Island. Results from these tests are shown in chapters 4 and 5. This thesis will briefly describe the background of Amchitka Island and will detail past studies, the methodology followed for this study, the results of the testing and will discuss the implications of these results.

## CHAPTER 2

### LITERATURE REVIEW

#### 2.1 Amchitka Island

The actual detonation of nuclear warheads started during the outbreak of the Cold War. A large number of nuclear weapons were tested at sites around the United States including Amchitka Island, Alaska. The Island is located in the Aleutian arc of Islands that comprise the emergent bodies of a long submarine ridge connecting North America and Asia. The Aleutian Islands form the dividing line between the Bering Sea and North Pacific Ocean. The island is located approximately 1340 miles west southwest from Anchorage, Alaska. Amchitka is situated nearly halfway to Asia, 765 miles west of the tip of the Alaska Peninsula and 870 miles east of Petropavlovsk, Kamchatka in the Russian Far East (Merritt, 1977). Amchitka Island is located at latitude  $51.5^{\circ}$  N and longitude  $179^{\circ}$  E (Dudley et al., 1977).

Amchitka was used as a forward fighter bomb base during World War II to reclaim the Japanese-occupied Aleutian Islands of Kiska and Attu. United States Military and Atomic Energy Commission operations have created severe toxic and radioactive waste problems on Amchitka Island. The U.S. Fish and Wildlife Service documented at least 33 toxic waste sites on the island, including areas with massive fuel spills, napalm bomb depositories and other unexploded ordnance, PCBs, solvents, and heavy metals (Merritt et al, 1977).

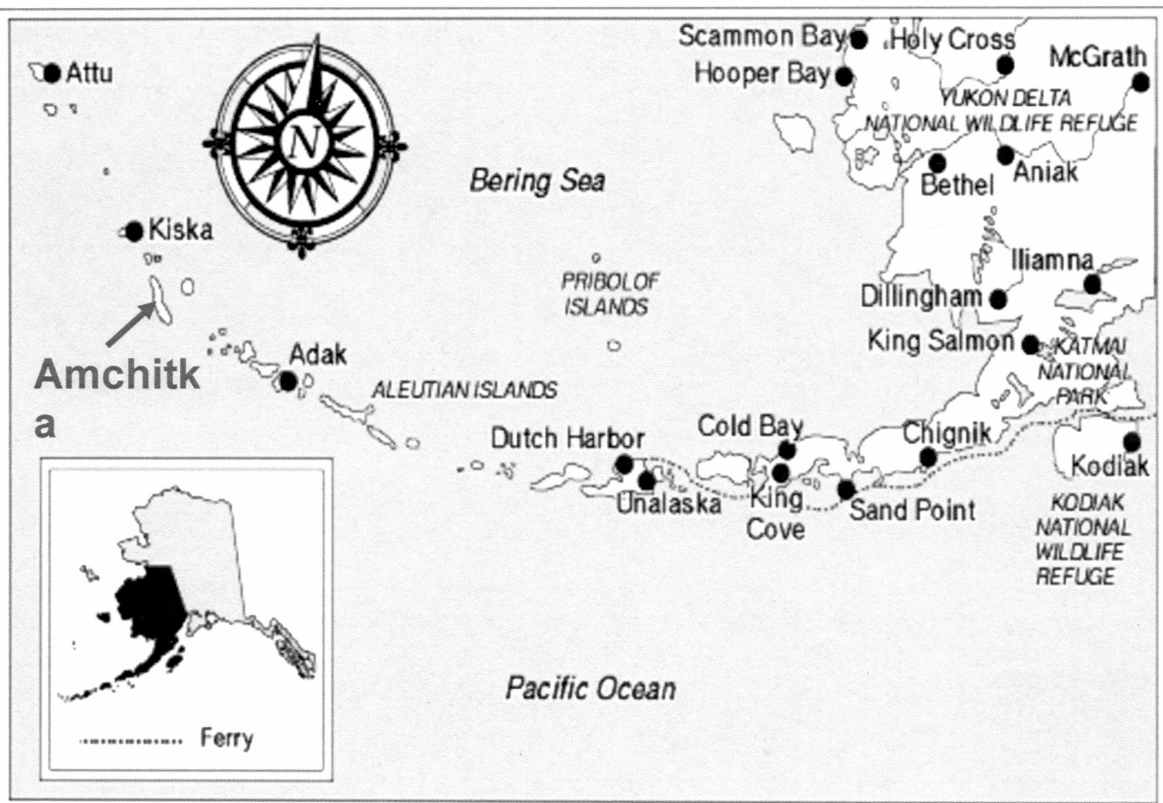


Figure 2.1. Amchitka Island position.

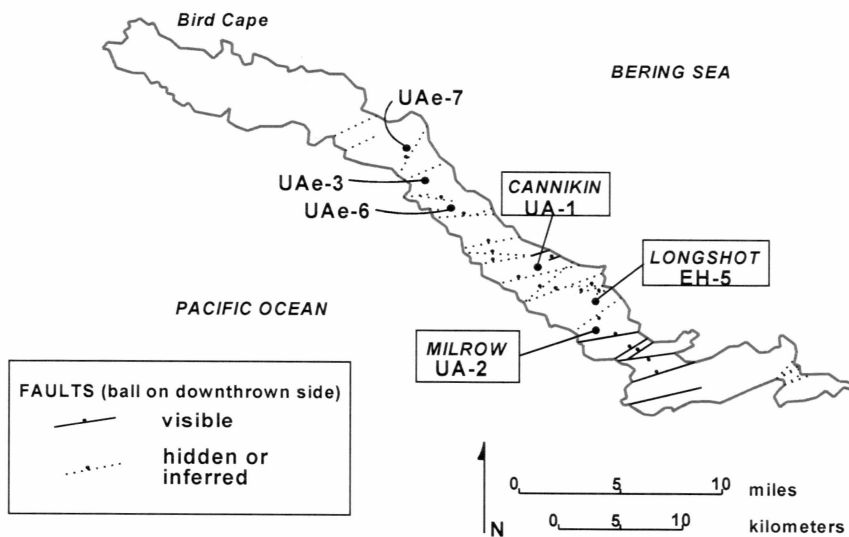


Figure 2.2. Map of Amchitka Island, Alaska- showing three nuclear detonation test sites.

## **2.2 Topography**

Through time Aleutian Islands had served as a home for many people. The region around Amchitka is sparsely populated. In the whole Aleutian Islands census division, which includes parts of Aleutian peninsula, there were only 11,942 people in 1990 (Bureau of the Census, 1990). The population of Amchitka Island according to the 1990 census was 25 mainly consisting of army personals (Bureau of the Census, 1990). However the Island is currently uninhabitable. The island is 40 miles long (65 km) and 1 to 4 miles wide (2 to 7 km). The island encompasses of 116 sq. miles of land and 161 sq. miles of water. It has a coastline with sea cliffs and grassy slopes up to 100 feet high surrounding the Island and the altitudes range from sea level to 1,160 feet. The topography of the Island consists of mountains, high and low plateaus (Dudley et al., 1977). The eastern part of the Island was very much comprised of shallow ponds and marshy lands covered by vegetation. Few lakes are located in the central lands. This area primarily consists of bedrock rubbles on ridges of a typical height of 60 m formed by freeze-thaw and high winds. It includes integrated drainage system and wind erosion. The western part is three miles spread with rocky and barren plateau of about 240 m high (Merritt, 1977).

## **2.3 Geological history**

The Island is divided into five landforms; a mountain segment, a high plateau, the Chitka point segment, lower plateaus and an intertidal bench (Powers et al., 1960). Amchitka Island was a geologic history representative of Aleutian Islands. The

rock structures of Amchitka island are one of the oldest which were formed during the early tertiary age (Carr et al., 1970), that has provided a record of deposition and alteration of more than 2300m of submarine pillow lavas, breccias and turbidities of basic to intermediate compositions. Pillow lavas were formed by the end of deposition of the Amchitka Island formation at the bottom a thick pile of monolithologic glassy breccia (Gard, 1971).

After the long volcanic activity (tertiary age) the banjo point formation was observed during late Eocene or early Oligocene time. During this time the basaltic debris shed from the volcanos nearby was deposited on the sea floor (Gard, 1971). Next came the mid-tertiary time where uplift, erosion and initiation of normal faulting occurred on Amchitka Island. This uplift has occurred along the western and central Aluetian ridge (Gates et al., 1954). At this time the Island stood higher above the sea level.

It was during the Pliocene time that basaltic and andesitic intrusions occurred. In the Pliocene time the island was still at a considerable height above the sea level. It was during this period two phases of minor intrusive activity occurred. Basaltic dikes, sills crop and andesite dikes are formed near the eastern end of the Island. Cross cutting of these rocks reveals that the andesite rock formations were younger among the basalts (Carr et al., 1970). The ground water flow in the Island occurs predominantly through fractures. There are many active faults in the Island.



## **2.4 Weather and Climate**

Frequent rains resulting in a lush and spongy landscape of maritime tundra inundate Amchitka. The annual range of mean daily temperature is 17 °F. The annual precipitation is 0.828 meters with the highest occurring July through January. Clear skies are rare at this Island but it is predominated throughout the year by clouds and fog (Armstrong, 1977, Merritt, 1977). There are no prevailing winds on Amchitka. In summers the winds tend to blow from the southwest due to semi permanent high pressure area that persists in the Gulf of Alaska in summer months (Merritt et al, 1977).

## **2.5 Tests Conducted on Amchitka Island**

In the early 1960s, Amchitka became a nuclear testing facility under the United States Atomic Energy Commission. Three underground nuclear explosions occurred in the 1960s and 1970s. The first among them was an 80-kiloton device named Long Shot. Long Shot was unique in two respects. It was the first underground event planned for an isolated island area, and it was the first nuclear experiment managed by the Department of Defense (DOD). This test was conducted on October 29, 1965 at a depth of 709.32 meters below the ground surface. The seismic energy produced from this test was measured as 5.75 on the Richter scale (Fuller, 1971; Kirkwood, 1975). Scientists detected radioactive leakage due to venting through the short chimney in the form of tritium and krypton-85 a few months after the test in freshwater ponds near ground zero

(EPA, 1997). Elevated levels of tritium were still measured in the Long Shot area in mud pits and ground water wells when the samples were taken in 1997 (EPA, 1997).

The second nuclear test that was performed on the Island was a 1 mega-ton tested named Milrow. It was detonated 1233 meters below the Island surface on October 2, 1969 (Merritt, 1977). The blast turned the surrounding sea to froth and forced geysers of mud and water from local streams and lakes 15.42 meters into the air. A large volume of rock, totaling about 6,900 cubic meters, fell from bluffs on the Bering coast (Merritt et al, 1977).

The final test conducted on the Island was named Cannikin, which was largest underground nuclear explosion conducted by the United States. The estimated 5 mega-ton device was detonated on November 6, 1971 at a depth of 1791 meters below the ground surface (Morris et al., 1972). A crater was formed 38 hours after the detonation, due to collapse of the explosion cavity, which slowly filled with surface water. The resulting lake, named Cannikin Lake, was 10 m deep and spread over a surface area of 30 acres (Gonzalez et al., 1974). The Cannikin projects main purpose was to test the Spartan anti-ballistic missile warhead.

Owing to the complex nature of the Island's subsurface, the relative remoteness of the Island, and the lack of complete understanding of the subsurface effects of the detonations, a traditional monitoring strategy for the Island (terrestrial contaminant

monitoring wells) will be difficult and costly to design and install. Thus, consideration is being given to designing a marine based monitoring program. No matter if the monitoring system is terrestrial based or marine based, we need to gain a better understanding of the mechanisms controlling the transport of radionuclides through the Amchitka subsurface.

## 2.6 Diffusion

Several tests on the diffusivities of granite and gneiss have been measured by others to determine the rock suitability for nuclear waste disposal (Skagius et al., 1986). Limited testing of igneous rocks has taken place. Due to the inherent heterogeneous nature of the pore structure in rock, it is not possible to give one precise value of diffusivity in rock materials even if taken samples are obtained in the close proximity to each other.

Transient concentration gradient driven diffusion transport is described by Fick's second law as follows:

$$F = D_e \frac{\partial \rho}{\partial x} \text{-----Eq.1}$$

where in  $F$  is the diffusion flux ( $\text{kg/m}^2/\text{s}$ ),  $D_e$  is the effective diffusion coefficient ( $\text{m}^2/\text{s}$ ), and  $\rho$  is the mass concentration ( $\text{kg/m}^3$ )

$$D_e = \varepsilon * D_m \text{-----Eq.2}$$

Where  $D_e$  is the Effective Diffusion Coefficient ( $m^2/s$ ),  $\varepsilon$  is formation factor, and  $D_m$  is the molecular diffusion coefficient ( $m^2/s$ ).

As shown in equation (1), effective diffusion is a function of formation factor. This factor is comprised of the descriptive pore space properties tortuosity, constructivity and porosity.

Numerous tests have been conducted by others to measure the effective diffusion coefficients for granitic rock associated with high level nuclear waste disposal. These tests are described subsequently.

Brown, 2000 conducted diffusion tests using non-reactive tracers on cannikin test site basalts and breccia. Brown used two different experimental procedures to measure the effective diffusion coefficient into basalts and breccias obtained from Amchitka Island. The first experimental method measured the diffusion of a conservative tracer (sodium bromide) from a cylindrical sample of core initially saturated with the tracer. Prior to beginning the diffusion experiment, all the outer surfaces of the sample except one surface is sealed with varathane to ensure that bromide tracer only diffuses through that exposed side. The saturated sample was immersed in ultra pure water and measurements of the tracer are taken with time using a bromide selective electrode.

The second test conducted by Brown, 2000 was a through diffusion test following the methodology similar to Feenstra et al., 1984 and Skagius et al., 1986. In this test sodium bromide was used as a tracer and was injected into the source cell. The receiving cell was filled with synthetic ground water. Samples were taken from the receiving cell at regular intervals of and analyzed with AA spectroscopy.

The conclusions obtained from these two experiments were that ions were diffusing slower through Amchitka breccia when compared to basalts regardless of experimental setup because of breccia having a smaller average pore diameter compared to basalts.

From the Br diffusion experiments data the following selectivity series can be established for groundwater conditions likely to be found at Cannikin test site (in order of decreasing diffusion rates): Cs(I)~ Br-> Pb(II). It was concluded that the migration of Cs(I) would be retarded due to diffusion of solute into and within the solid matrix. Finally it was shown that the values of diffusion coefficients differed by approximately an order of magnitude between the two experimental methods (Brown, 2000).

One option for disposal of contaminated water from uranium mine was by deep well injection into fractured rock. An analytical model was developed to simulate the radial movement of the contaminants under steady flow conditions in a planar

fracture (Tang et al. 1981, and Frind, 1982). For this modeling effort the effective diffusion coefficients for the sand stone rock measured in the laboratory was known as through diffusion tests. In this paper for the determination of diffusion coefficients Feenstra et.al, 1984 proposed a small two compartment reactor, with one compartment filled with deionized water and the other with 2M sodium chloride solution to conduct a through diffusion test. The liquid levels in both the chambers were kept same. From the mass transfer of chloride in this diffusion test, the effective diffusion coefficient was calculated as follows (Feenstra et al., 1984).

$$\frac{D'_{(t_1-t_2)} AC^A}{L} = \frac{V^B (C_{t_2}^B - C_{t_1}^B)}{t_2 - t_1} \quad \text{----- Eq (3)}$$

where  $D'_{(t_1-t_2)}$  is the effective diffusion coefficient ( $L^2/T$ ) measured between time  $t_1$  and  $t_2$ ,  $C^A$  is the concentration in compartment A ( $M/L^3$ ),  $C^B$  is the concentration in compartment B ( $M/L^3$ ),  $V^B$  is the volume of solution in compartment B ( $L^3$ ),  $A$  is the area of rock disk ( $L^2$ ),  $L$  is the thickness of the rock disk ( $L$ ), and  $t$  is the time ( $T$ ).

The effective diffusion coefficient of a sample of sandstone rock was found to be in the range of  $3.4 \times 10^{-12}$  to  $3.2 \times 10^{-11} \text{ m}^2/\text{sec}$  with a mean value of  $1.5 \times 10^{-11} \text{ m}^2/\text{sec}$  (Feenstra et al, 1984).

Bradbury et al., 1982 carried out diffusion measurements using iodide as a tracer on a number of granite samples from four different regions of the United Kingdom.

Two parameters characterizing diffusion through porous rock, intrinsic diffusion coefficient and the rock capacity factor were determined where the rock capacity factor ( $\alpha$ ) is given as:

$$\alpha = \varepsilon + \rho K$$

where  $\varepsilon$  is water-accessible connected porosity,  $\rho$  is rock density and  $K$  is the distribution ration, which is concentration dependent for some nuclides.

A through diffusion methodology similar to Feenstra et al., (1984) was used by these researchers to determine the diffusion coefficients of the rocks. Firstly the rock sample was saturated with  $\text{KNO}_3$  solution and was sealed between rock holders separating a tracer source cell from a receiving cell. The source cell was filled with 1 M potassium iodide (KI) solution and the receiving cell was kept at an equal depth with an isotonic solution of  $\text{KNO}_3$ . Isotonic solution was used to eliminate the possibility of osmotic driven fluxes and also to ensure that iodide diffusion was measured and not the KI diffusion. The influence of dead-end porosity, which comprises cross-linked pores and pores closed at one end, on diffusion was observed. The diffusion coefficients of these samples were found to be ranging from  $1.4 \times 10^{-12}$  to  $3.3 \times 10^{-14} \text{ m}^2/\text{s}$  (Bradbury et al., 1982).

In Sweden and other countries nuclear wastes were disposed of by placing them deep into the underground repositories in crystalline rock (Skagius et. al, 1986). To determine the suitability of the host rock to contain these materials diffusion tests were

conducted on the non-sorbing species iodide, uranium and Cr-EDTA. The porosity of the rock sample was measured by two methods. The first method measured the difference in the mass between vacuum and oven dried samples of rock. The second method for determining the porosity was by leaching after the diffusion experiment. The amount of compound present in each sample was determined by leaching the component from the sample using distilled water. The leaching process was performed until the tracer concentration in the leach solution was constant in time. The porosity was determined by mass balance (Skagius et al., 1986). Through diffusion experiment performed by Skagius et al., (1986) were conducted in the same magnitude as described by Bradbury et al., (1982). The through diffusion test was carried out and the graphs were plotted between concentration of iodide and Cr-EDTA versus time as described by Bradbury et al., 1982. The effective diffusion coefficients were determined by this diffusion method. To balance for the ionic strengths sodium nitrate was added to the lower concentration cell. The effective diffusion coefficients determined ranged from  $1 \times 10^{-14}$  to  $7 \times 10^{-13}$   $\text{m}^2/\text{s}$  (Skagius et al., 1986).

The diffusivity of sorbing species on rocks materials from Sweden were studied by Skagius et al. (1982) and effective diffusion coefficient for example cesium and strontium was determined as in the order of  $10^{-12}$  to  $10^{-11}$   $\text{m}^2/\text{s}$ . Diffusion of nuclides into the pores can act as a retarding and diluting mechanism by removing the nuclides from the flowing groundwater in the fissures (Skagius et al., 1982).



Skagius et al., 1988 conducted two experiments, the first test was conducted using a methodology known as in-diffusion, where in two samples are taken and kept in cesium and strontium solution respectively. The samples are removed from strontium and cesium solution after 385 and 470 days respectively. From the center of each sample a small core is drilled out and is cut into two halves. One half is grounded. The amount of cesium or strontium in the grounded material from each of the sections is determined by atomic absorption spectrometer on the dissolved aqueous phase. The second test followed through diffusion methodology that has been explained by Feenstra et al., 1984 and Skagius et al., 1986 shown in fig 3.1. In this test, cesium solution and strontium solution are used as a tracer. The tests were conducted for 315 days for cesium and 412 days for strontium. The samples were removed from the diffusion cell are grounded and concentration of cesium and strontium is determined using atomic absorption spectrometry to give the concentration profile in the samples. The effective diffusive coefficients measured were ranging from  $5.3 \times 10^{-13} \text{ m}^2/\text{s}$  to  $7 \times 10^{-13} \text{ m}^2/\text{s}$  (Skagius et al, 1988).

Heath et al.,(1992) performed studies on blocks and cores of El Berrocal granite intersected by hydrogeologically-active fractures to determine the extent to which diffusion of natural radionuclides has taken place from fractures into the rock matrix. The authors also studied the microstructural controls of diffusion and also studied to determine the diffusion depth in rock adjacent to fractures is sufficiently limited to undermine the existing diffusion models. The researchers collected samples from sites in

Spain, Canada and Sweden. The physical, dynamic and geochemical properties of the collected samples were integrated. The cores collected from Spain showed evidence of water movement through open fractures free diffusion through solid rock matrix does not appear to have taken place. The results showed that matrix diffusion, in many granite rocks, does not take place as freely as previous models have implied. The host formation with a low fracture density was selected and water movement along fractures with high flow velocity leads to the restriction of nuclides to the walls of fracture. The results implied that in many granitic rocks the matrix diffusion is limited to a zone, which could be very few centimeters from the fractures, and the diffusion rate is higher near that fracture compared to the deeper zones.

Barone et al., 1989 showed that the efficiency of matrix diffusion as a retardation process for the transport of the contaminants through the fractured media in the natural environment was smaller when compared with the laboratory experiments conducted on stress-released samples. Laboratory experiments had been conducted in which distilled water was in contact with intact shale having a higher concentration of chloride in their pore water. This experimental model consists of a plexiglas cylinder of approximately 11 cm in length. A rock sample was cut in a cylindrical shape of length 7.1 cm and was made to fit into the cylinder. The inner sides of the cylinder are lined with rubber to keep the rock moist. Water was poured into the cylinder and the upper part is closed with plexiglas and fitted with polyethylene cap plate. The sample is maintained at laboratory temperature of 22<sup>0</sup> C for a period of 65 days. Chloride is allowed to diffuse out

of the shale into the distilled water reservoir for 65 days. The rock sample is taken out and cut into eight segments followed by drying at  $100^{\circ}\text{C}$  for 48 hrs. The average moisture content is determined after drying. The sample is pulverized and ground and centrifuged for 30minutes at 2500rpm and then analyzed for chloride concentration. Finally the diffusion coefficient of chloride was calculated using the values of moisture content. The effective diffusion coefficient measured ranged from  $1.4 \times 10^{-6}$  to  $1.6 \times 10^{-6}$   $\text{m}^2/\text{s}$  (Barone et al., 1989).

In summary, this literature review found other researchers to be using several different methods for determining the effective diffusion coefficients. One of the more common method used for these measurements appeared to be the through diffusion test. The effective diffusion coefficients for several different rock types are reported in the literature. The table below summarizes these values.

Table 2.1 Reported values of Effective Diffusion Coefficients ( $D_e$ ).

ROCK TYPE	TRACER	$D_e$ in $m^2/s$	REFERENCE
Sandstone	Sodium Chloride	$3.4 \times 10^{-12}$ - $3.2 \times 10^{-11}$	Feenstra et al., 1984
Granite	Iodide	$1.4 \times 10^{-12}$ - $3.3 \times 10^{-14}$	Bradbury et al., 1982
Crystalline	Iodide	$1 \times 10^{-14}$ - $7 \times$ $10^{-13}$	Skagius et al., 1986
Biotite Gneiss	Cesium and Strontium solution	$5.3 \times 10^{-13} m^2/s$ to $7 \times 10^{-13}$	Skagius et al., 1988
Sandstone	Cesium and Strontium solution	$10^{-11}$ - $10^{-10}$	Bradbury et al., 1986
Granite	Cesium chloride or Strontium chloride	$10^{-7}$ - $10^{-8}$	Tsukamoto et al., 1990
Shale	Chloride	$1.4 \times 10^{-6}$ to $1.6 \times 10^{-6}$	Barone et al., 1989
Basalt	Cesium	$1.5 \times 10^{-13}$	Santo et al., 1997
Granddiorite	Cesium	$1.4 \times 10^{-12}$	Santo et al., 1997

This literature review had found the various values of porosities of different rock types by different researchers. These values were found by using different methods. The table below summarizes these values.

Table 2.2. Reported values of Porosities

Rock type	Porosity	Reference
Crystalline	0.14-1.46	Skagius et al., 1986
Granite	0.014	Tsukamoto et al., 1990
Sandstone	0.10	Feenstra et al., 1984
Granite	0.45-0.6	Schild et al., 2001
Mica Gneiss	0.2-0.8	Holttä et al., 1996

## **CHAPTER 3**

### **METHODOLOGY**

The detonation of nuclear weapon releases a suitable amount of radionuclides to the environment. If the detonation was carried out in subsurface, the released radionuclides become a source of groundwater contamination. To measure  $D_e$ , four different tests were conducted on two samples of andesite rock from core extracted from the Island during the 1960s or early 1970s in preparation for underground nuclear testing. Two of the diffusion tests conducted in this research followed the through diffusion methodology described previously and two tests followed a methodology known as elution. The conservative tracer used in this study was iodide in the form of potassium iodide (KI). This tracer was chosen due to its conservative nature. Others have also used this tracer successfully for measuring effective diffusions (Feenstra et al., 1984). Iodide concentration during the testing was measured using the leuco crystal violet method (Standard Methods 4500-1D, 1995). The components of the methodology followed will be described subsequently.

#### **3.1 Leuco Crystal Violet Method**

The leuco violet method of determining iodide concentrations is a colorimetric method (Standard Methods 4500-1D, 1995). Firstly, iodide was selectively oxidized to iodine. The reduced iodine reacts instantaneously with the colorless indicator reagent N,N-dimethylaniline, known as leuco crystal violet, and produces a colored violet

solution. The color in the solution was stable for a period of time and adheres to Beer's Law allowing for the determination of absorbance values over a wide range of iodine concentrations. Absorbance was measured using spectrophotometer at a wavelength of 592 nm. In this procedure, a solution of citric acid buffer was used to stabilize pH. This buffer solution was also used in the through diffusion tests to equalize solution densities in an attempt to reduce advective transport of tracer through the rock sample.

### **3.2 Through Diffusion**

From the collection of rock core removed from the Island, a core of andesite was selected in such a way that there are no cracks through its length and diameter. Two slices of the core were obtained. The first slice of core measured 3 mm thick and 76.2 mm in diameter. The second slice was 4.5 mm thick and 9 cm in diameter. The position of the rock slices on the core prior to cutting was separated by a distance of 18 cms.

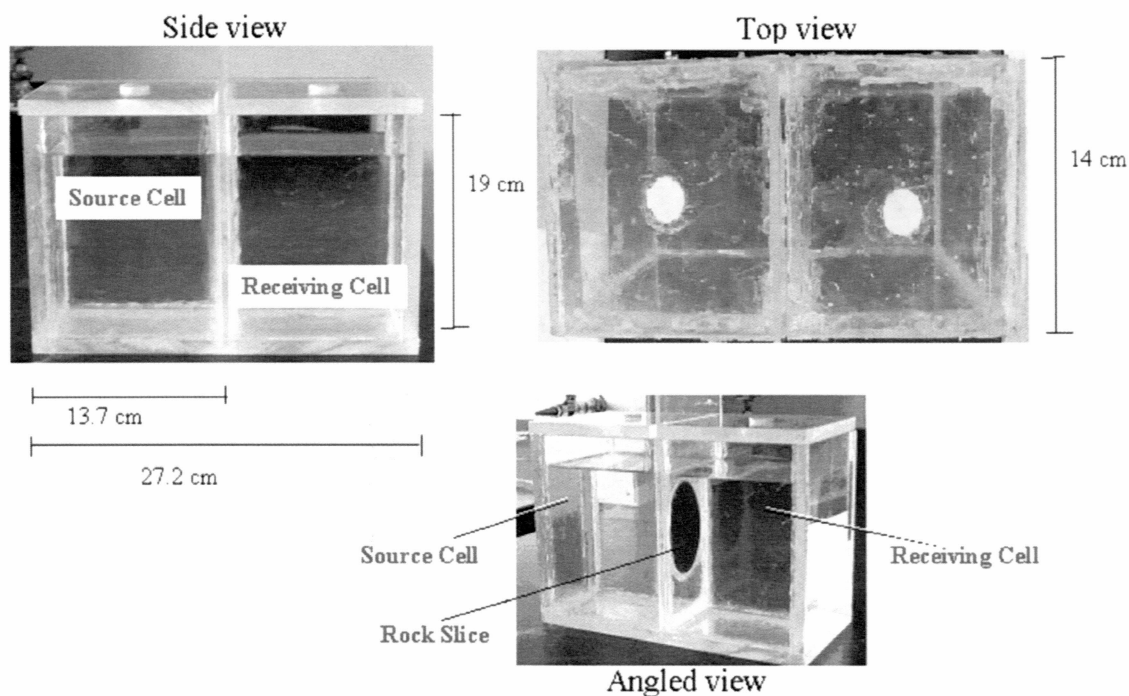


Figure 3.1 Two cell Diffusion reactor

Figure 3.1 shows a schematic and picture of the reactor used in this study. The reactor was constructed of 1.27 cm thick acrylic plastic and divided into two cells with a 0.762 cm thick acrylic partition that contains the rock sample. Roughly at the middle point of the reactor, the sides and bottom are grooved to accommodate the divider. This design allows reuse of the reactor. Silicon sealant was used to seal joints throughout the reactor and to seal the rock slices into the divider.

Once a core slice is secured in the reactor, the rock is saturated with deionized water by filling the source cell with deionized water to a water level above the top of the rock slice. A small volume of deionized water is also placed in the receiving cell, however the depth of water in this cell is below the bottom of the rock slice. The



reactor was covered and left undisturbed. Saturation was confirmed by the appearance of water on the receiving side of the rock slice. Once water appeared uniformly across the face of the receiving side of the rock slice, the receiving cell was filled with deionized water to a water level above the top of the rock slice. This method of saturating the rock slice not only reduced the possibility of entrapping air in the rock's pore space, but also allowed for the identification of fractures in the rock that would result in unrepresentative relatively high rates of diffusion through the rock. A small fracture was identified by this method in the first rock slice tested (sample 1). Silicon sealant was applied to this small discontinuity, to reduce the influence of this region on the measurement of effective diffusion in this sample.

An initial 0.5 molar concentration of potassium iodide (63.13 moles/liter of iodide) was used in the source cell for the through diffusion test on sample A. For this test only deionized water was present in the receiving cell initially. Both cells were stirred with a magnetic stir bar. After the initiation of the tracer into the reactor, frequent samples were taken from both the source cell and the receiving cell. For the through diffusion test on sample 2 potassium iodide concentration was reduced to 0.3 moles per liter (37.87 moles/liter iodide). Also in the through diffusion test for rock sample 2, a solution of citric acid buffer was used to equalize the densities of the solutions in the source and receiving cells. Citric acid buffer was used so as not to interfere with the leuco crystal violet method used to measure iodide.

### 3.3 Elution Test

As the through diffusion test progresses the concentration in the receiving cell will approach the concentration in the source cell until equilibrium was obtained. At equilibrium the concentration of iodide in the water contained in the rock pores will equal the concentration in both reactor cells. After a sufficient time to assure that equilibrium has truly been obtained, the rock sample was extracted from the reactor and immersed into a reactor containing one liter of deionized water allowing for diffusion of iodide from the rock pore space into the deionized water. This solution was not stirred, which, as will be discussed later in the thesis, was an oversight in this methodology. Measurement are frequently taken from this reactor and measured for iodide.

### 3.4 Porosity Measurements

Porosity was determined by two methods. For rock sample 1, the porosity was calculated with a mass balance using results from the through diffusion and elution tests. Porosity for rock sample 2 was measured by both a mass balance and by saturated versus dry weight measurements. Porosity by the method is determined from the following equation:

$$\phi = \frac{\rho_w - \rho_D}{\rho^*} \quad \text{-----Eq .4}$$

Where  $\rho_D$  is dry density (mass/volume),  $\rho_w$  is wet density (mass/volume), and  $\rho^*$  is 1000 kg/m<sup>3</sup> (water).

Mass balance determination of porosity requires the initial concentration of iodide contained in the rock pore space prior to the elution test and the final concentration of iodide in the rock pore space once equilibrium has been obtained in the elution test. The equation is as follows:

$$\phi = \frac{\rho_f}{\rho_0 * V_s} \text{-----Eq(5)}$$

Where  $\rho_f$  is final concentration (mgs/l),  $\rho_0$  is initial concentration (mgs/l),  $V_s$  is the volume of the sample (cm<sup>3</sup>)

### 3.5 Control Tests

The first control test to be performed was the determination of the background concentration of iodide in the rock samples. For this test, samples of the rock core were immersed in deionized water. Samples of the solution were measured for iodide over time. The sorption of iodide onto the reactor materials was also tested. For this test, silicon and acrylic samples of known dimensions were immersed into 0.3 molar solution of potassium iodide (37.87 moles/liter iodide). The acrylic sample was 2.5 x 2.5 cm and the silicon was a spherical ball of approximately 3.4 cm in diameter. Samples of the solution were taken over time and measured for iodide. Possible diffusion of iodide through reactor materials was also measured. This procedure was a duplication

of the through diffusion test described previously, only with a solid divider separating the source and receiving cells instead of a divider containing a rock sample.

## **CHAPTER 4**

### **RESULTS**

To estimate the effective diffusion coefficient four different tests were conducted; two through diffusion tests and two elution tests. To determine the effective diffusion coefficient from these measurements, porosity was determined for each sample. In addition, to determine the sorptive capacity of the reactor materials, sorption tests were performed on the acrylic and the silicon sealant used to make the reactor watertight and to seal the divider between the two cells of the reactor. Finally, a control test was run on the reactor materials to assure that diffusion was not occurring into and through the sealant and acrylic. This chapter presents the results of these tests.

#### **4.1 Sample 1 Through Diffusion Test**

As described previously, the first through diffusion test was conducted on a 76.2 mm diameter and 3 mm thick piece of andesite rock core. The results from this test are shown in Figure 5.1

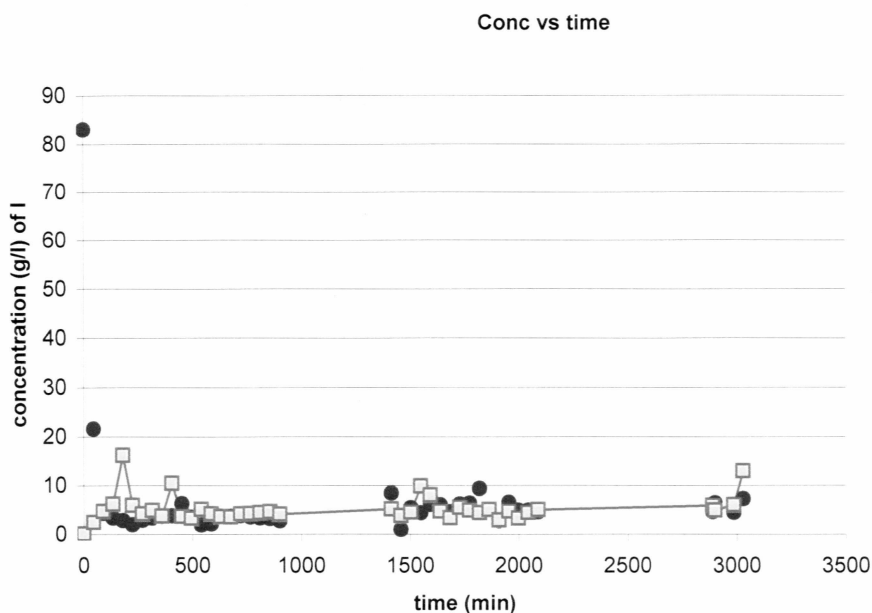


Figure 4.1. Concentration of iodide as a function of time in the source and receiving cells obtained from a through diffusion test on rock sample 1.

This first through diffusion experiment was unsuccessful. While the data shows a decrease in the source cell concentration, there was no associated increase in receiving cell concentration. The exact cause of the test failing was not known. However during the experiment an unexplained color change from a clear solution to a reddish brown solution occurred in the source cell. Subsequent tests showed this color change to be possible due to a photochemical reaction. Reactors were wrapped with aluminum foil to eliminate the possibility of this reaction occurring in future tests. Further investigation into the cause and effect of this color change were not pursued. Concentration values in both the cells also show oscillations between high and low

concentrations. Through diffusion tests on sample 2 show this same pattern of oscillation. A reasonable explanation for this pattern cannot be derived. The reason this through diffusion test failed can most likely be attributed to experimental error in measuring iodide concentrations in the two reactors as well as some possible photochemical reaction that cannot be currently explained.

#### 4.2 Sample 2 Through Diffusion Test

The same procedure was followed in this test as in the through diffusion test for sample 1 except for covering the reactor to eliminate a photochemical reaction which was previously discussed. Figure 4.2 shows the results from this through diffusion test.

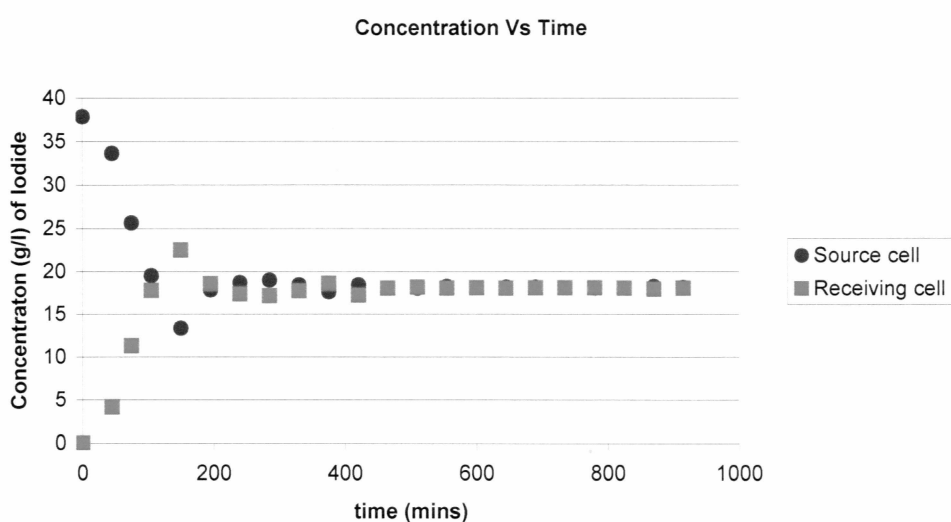


Figure 4.2. Concentration of iodide as a function of time in the source and receiving cells obtained from a through diffusion test on rock sample 2.

Results from the through diffusion test on sample 2 are more consistent with characteristic through diffusion curves. As noted in the results from the through diffusion test on sample 1, oscillations of the concentrations in both cells are once again evident in these results. However, these oscillations dampen in a little over 200 minutes. Counter to the first test, there was no noticeable solution color change in either cell.

#### **4.3 Sample 1 Elution Test**

To perform an elution test on Sample 1, the core slice was extracted from the through diffusion reactor at the termination of the through diffusion test. During the extraction of the core slice, the slice broke into two pieces. Both pieces of sample 1 were immersed in one liter of deionized water. Because of the broken sample the results obtained from the elution test may be compromised due to the small increase in surface area available for diffusion of iodide out of the rock sample. Results from this elution test are shown in Figure 4.3. As shown in this figure, the deviation of the datum point at approximately 1400 minutes was most likely due to measurement errors.



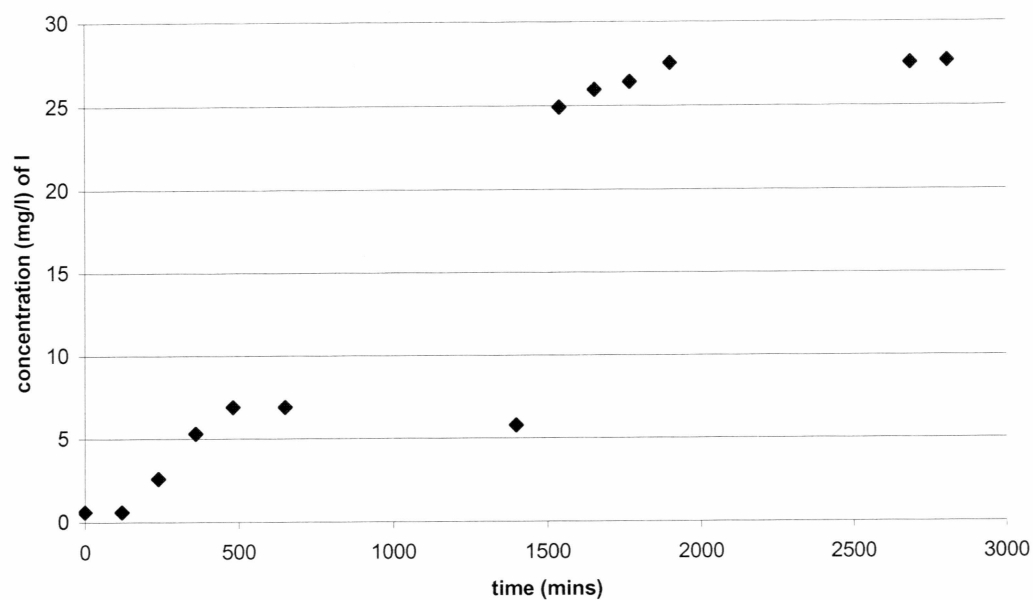


Figure 4.3. Concentration of iodide as a function of time obtained from an elution test on rock sample 1.

#### 4.4 Sample 2 Elution Test

Results from the elution test on rock sample 2 are shown in Figure 4.4.

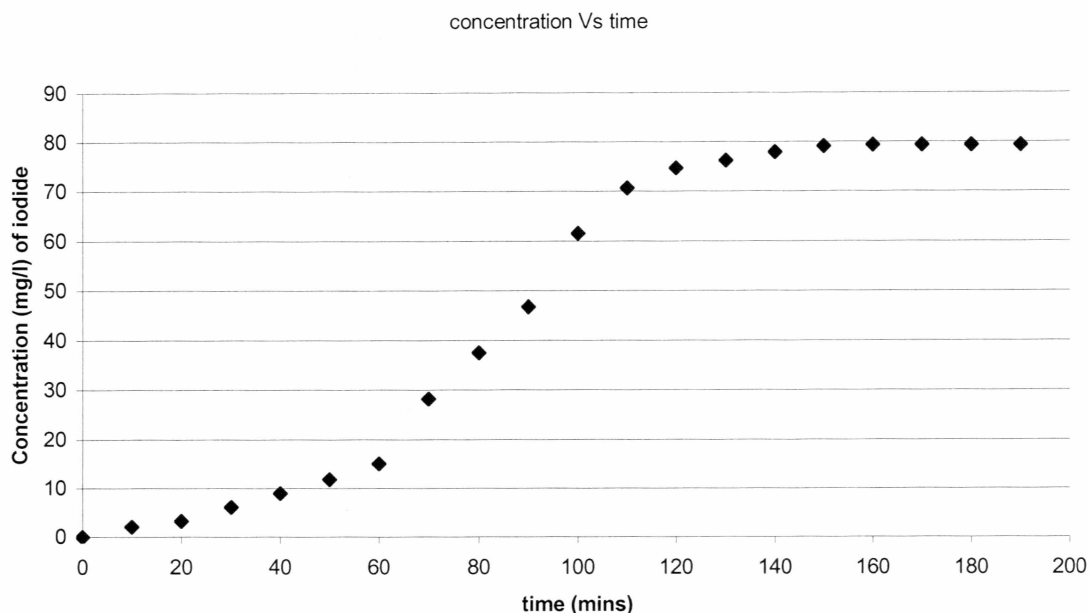


Figure 4.4. Concentration of iodide as a function of time obtained from an elution test on rock sample 2.

Comparing elution test results from both of the rock slices (Figures 4.3 and 4.4) a difference in the nature of the two curves was noted. The shape of the curve for sample 2 has a distinct “S” shape, while the curve for sample 1 does not show this trend. As noted in the previous chapter, neither elution test was stirred, thus the time required for each solution to reach equilibrium during the elution test was longer in comparison to if the solution had been stirred. Most likely the difference between the two curves was a function of where the solution samples were taken from the reactor to be measured for iodide. The resulting curve for sample 1 is more characteristic with what one would expect to see during an elution test.

## 4.5 Porosity

As described previously, two different methods were used to measure the porosity of the core slices: a mass balance procedure and a measurement of the mass of water lost during drying of the rock sample. The mass balance method applied to the sample 1 was complicated owing to the questionable concentration data obtained from the through diffusion test. To make this calculation the final concentration resulting from the through diffusion test has to be assumed ( $\rho_o$  in Equation 5, Chapter 3). To make this assumption, consider that the concentrations in both cells and in the pore water in the rock slice once equilibrium has been obtained in the through diffusion test are equal. Referring to Figure 3.1, the volume of each cell in the through diffusion reactor is roughly the same volume. Thus,  $\rho_o$  is roughly one-half of the initial concentration of iodide placed in the source cell, or 42 g/L. Results from the through diffusion test on sample 2 confirms this assumption. The concentration of iodide at the end of the elution test,  $\rho_f$  is 27.56 mg/L. Thus, from Equation (5), the calculated porosity for sample 1 is 0.047. Using the same methodology for sample 2 with  $\rho_o$  equal to 18.1 g/L and  $\rho_f$  equal to 79.4 mg/L, a porosity of 0.153 results. A porosity of 0.041 was determined by wet and dry mass measurements for rock sample 2. The difference between the two methods for rock sample 2 is most likely due to incomplete drying. Differences in porosity depending on the technique used for the measurement are not uncommon. Skagius et al., 1986 showed up to an order of magnitude difference between porosities measured by two different methods. The difference in porosity values for various rock samples is shown in

literature review in Table 2. Table 4.1 summarizes the porosity results for the two rock samples.

Table 4.1 Porosity measurements of two rock samples

Test	Porosity of rock sample	
	Rock 1	Rock 2
Weight measurements	-	0.041
Mass balance	0.047	0.153

#### 4.6 Control Tests

The first control test performed was to determine the background concentration of iodide in the andesite rock. Measurements taken during this leaching test indicated that no iodide was leaching from the rock sample. The sorptive capacity of the reactor materials was tested resulting in approximately  $2.7 \text{ g/m}^2$  of iodide sorbing onto the silicon sealant with an initial concentration of  $37.878 \text{ g/l}$  and final concentration observed is  $37.77 \text{ g/l}$ . There was no indication of a sorption of iodide onto the acrylic reactor material. Measurements taken to determine if iodide could diffuse through the reactor materials resulted in no indication that diffusion through these materials takes place during the 48 hours that the test was conducted.

## **CHAPTER 5**

### **DISCUSSION**

The purpose of this study was to measure the effective diffusion coefficient of andesite rock obtained from Amchitka Island, Alaska. In this chapter the results from the diffusion tests are discussed. Effective diffusion coefficients are estimated from the through diffusion and elution test results using a numerical solution to Fick's Second Law. The formulation of this model is described. Next the estimation of the effective diffusion coefficients is discussed. These measured coefficients are discussed and compared to effective diffusion coefficients determined in other studies for different rock types.

#### **5.1 Numerical Estimation of Effective Diffusion Coefficients**

Owing to the changing boundary conditions with time for both the through diffusion test and the elution test, there was no analytical solution to Fick's Second Law Eq (1). Thus, a numerical solution was required to determine the effective diffusion coefficient resulting from these tests. For this research, a forward in time, centered in space finite difference approach was used to solve the partial differential equation. The finite difference solution is as follows:

$$\rho_i^{t+\Delta t} = C\rho_{i-1}^t + (1-2C)\rho_i^t + C\rho_{i+1}^t \quad \text{-----Eq (6)}$$

In Eq (6)

$$C = \frac{D_e \Delta t}{(\Delta x)^2}$$

where  $\rho_i^t$  is mass concentration in cell  $i$  at time  $t$ ,  $C$  is constant,  $\Delta t$  is time step,  $\Delta x$  is cell width, and  $D_e$  is effective diffusion coefficient.

An example of the finite difference grid for the through diffusion test was shown in Figure 5.1.

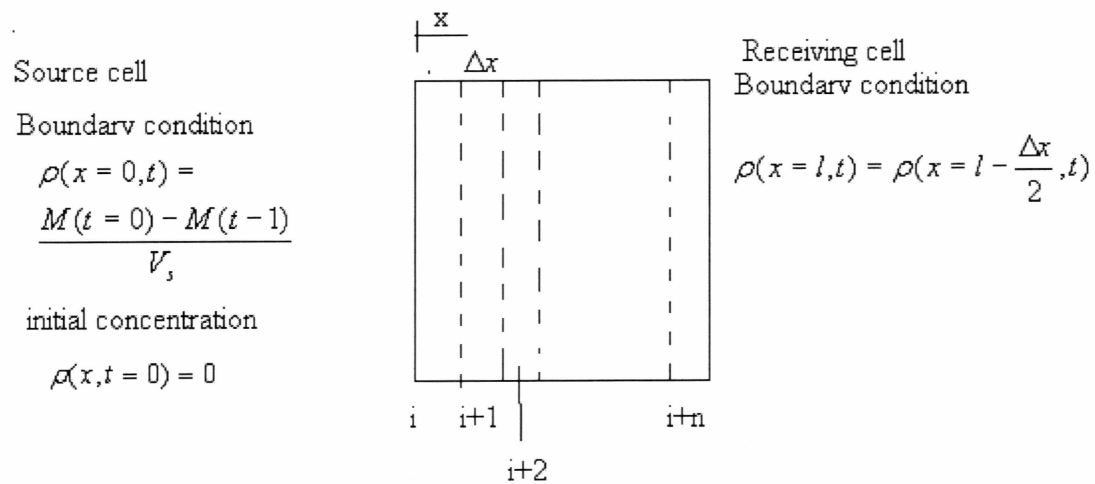


Figure 5.1. Finite element grid and boundary and initial conditions for the numerical solution to the Fick's Second Law applied to the through diffusion test.

A mass balance approach was used to obtain the source cell boundary condition. For the through diffusion test, at each time step the total amount of mass that has diffused into the rock and into the receiving cell was calculated. The calculated value is subtracted from the total mass placed into the source cell at the initiation of the test. The porosity of the rock core was required for this calculation. The boundary condition in the receiving cell was variable as well. For this boundary condition, an assumption was made that the concentration in the rock core in the finite difference cell closest to the reactor's receiving cell was equal to the concentration in the receiving cell. This assumption was valid if the finite difference cells are sufficiently small. A sensitivity analysis was required to determine how small the cells should be to provide a reasonable simulation of the diffusion process.

Methods used to determine the boundary conditions for the elution test at each time step are similar to the method used for the through diffusion solution. For this solution, a mass balance was used to determine the mass of tracer that has diffused out of the rock slice with each time step. This value was then subtracted from the initial mass in the rock. Concentration as a function of time in the reservoir was calculated knowing the volume of deionized water in the reservoir. An example of the finite element grid for the elution test was shown in Figure 5.2. The numerical codes for both solutions are contained in Appendix B.

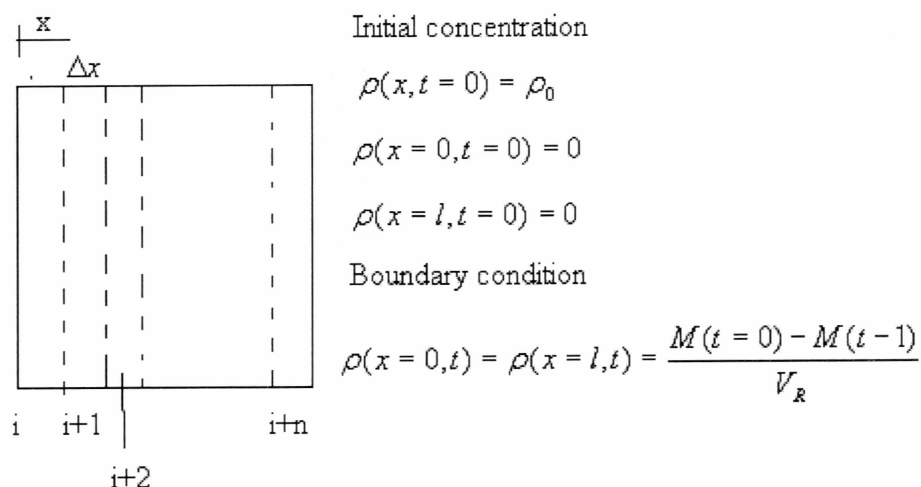


Figure 5.2. Finite element grid and boundary and initial conditions for the numerical solution to the Fick's Second Law applied to the elution test.

## 5.2 Sample 2 Through Diffusion Test

Adjusting the effective diffusion coefficient in the numerical solution described above the model results can be compared to the experimental data. A best fit was obtained using a mean square fit routine. A value for the effective diffusion coefficient that results from this best fit is  $1.23 \times 10^{-9} \text{ m}^2/\text{s}$ . The result of this comparison for the source cell was shown in Figure 5.3.



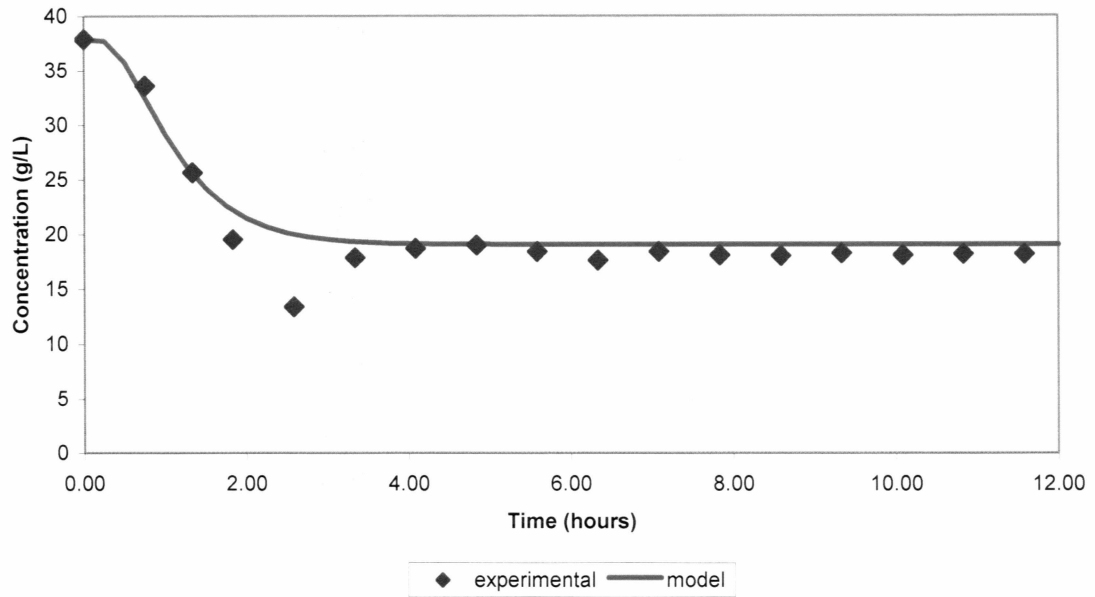


Figure 5.3. Best fit of numerical model results to source cell experimental data for the through diffusion test on sample 2.

This model fit routine was also applied to the receiving cell experimental data. From this effort a value of  $1.28 \times 10^{-9} \text{ m}^2/\text{s}$  is observed. The result of this comparison was shown in Figure 5.4.

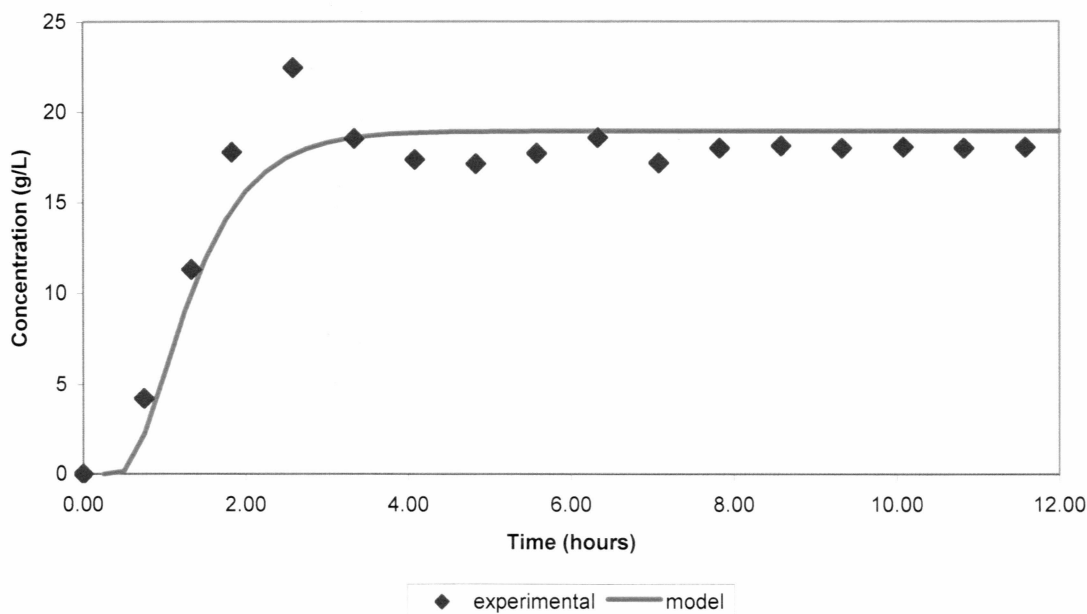


Figure 5.4. Best fit of numerical model results to receiving cell experimental data for the through diffusion test on sample 2.

As shown in both the above figures, the numerical model results adequately fit the experimental data from both cells in the through diffusion test. Also, the effective diffusion coefficients obtained from the best fit of the model to the data in both cells are comparable. Close examination of the model results for both cells shows a deviation of the model from the experimental results due to the unexplainable oscillation in the experimental results and a slight deviation of the results from the experimental data in the later stages of the test. The slightly greater value of concentration calculated by the model during this later time was most likely due to the sorption of the iodide onto the silicon sealant as described in Chapter 4. If a rough estimate of the total sealant surface area was made by assuming that the surface of the sealant along all sealed joints was

rectangular in shape with a width of the rectangular estimated to be approximately 0.7 cm, the initial mass balances with the sum of the final masses contained in the source cell, receiving cell, rock pore space, and sorbed onto the sealant. No other sources of sorbent materials (acrylic or rock) were found from the control tests conducted.

An interesting comparison was made between the molecular diffusion coefficient and the measured effective diffusion coefficient presented above. Skagius et al. (1986) reports a value of  $1.615 \times 10^{-9} \text{ m}^2/\text{s}$ . This value to the measured effective diffusion coefficient by introducing a formation factor, which was simple the ratio of effective diffusion coefficient to the molecular diffusion coefficient. This factor incorporates the properties of the rock that reduce the mass flux of a tracer diffusing through the rock. Such properties include tortuosity, constrictivity, and porosity. Tortuosity is simple the extended path length invoked by the non straight pathways developed through the pore space. Constrictivity addresses the non uniform diameter of the pore throats. Porosity is, of coarse, the volume of pore space in comparison to the bulk volume. Different formulations of these factors have been pesented in the literature. One such formulation presented by Marsily (1993) is as follows:

$$F = \frac{D_e}{D_m} = \frac{\phi * \delta_D}{\tau^2} \text{ ----- Eq (7)}$$

In Equation (7) F is formation factor,  $D_e$  is the effective diffusion coefficient ( $\text{m}^2/\text{s}$ ),

$D_m$  is molecular diffusion coefficient (m/s),  $\phi$  is porosity,  $\delta$  is constructrivity, and  $\tau$  is tortuosity. The resulting formation factor for rock sample B is 0.76. A value for this factor close to unity indicates that there was little retarding effect of the rock properties on diffusion.

### 5.3 Sample 2 Elution Test

The numerical model for the elution test can be compared to the experimental results for this test in the same manner as described for the through diffusion test. The porosity of the rock was determined by the mass balance method described in Section 4.5 was used for this comparison. As discussed in Section 4.4, the solution was not stirred during the elution test. This oversight resulted in data that does not compare favorable to what would be expected from such a test. To Compare the numerical model to the experimental data for this test, an assumption was made that the maximum concentration in the solution that was reached once the solution has obtained equilibrium does not occur at any later time than what was shown in the results (refer to Figure 4.4). This assumption is valid given the molecular diffusion from the rock face to the sampling point distant from the rock face that had to occur once the tracer diffused out of the rock. If the reactor had been stirred equilibrium would have most likely been obtained earlier than what the data shows. If this assumption was accepted then the numerical model is best fit to data obtained in the later stages of the test is opposed to the early data.

Fitting the model to the data in this fashion results in a minimum diffusion coefficient of  $1.23 \times 10^{-9} \text{ m}^2/\text{s}$ . This coefficient was considered a minimum since the actual rate of diffusion is not known. If a diffusion coefficient was chosen that was less than this value, then the numerical model results do not adequately fit the data for the later stages of the test, which according to the assumption made was not acceptable. The comparison between the numerical model results and the experimental data was shown in Figure 5.5

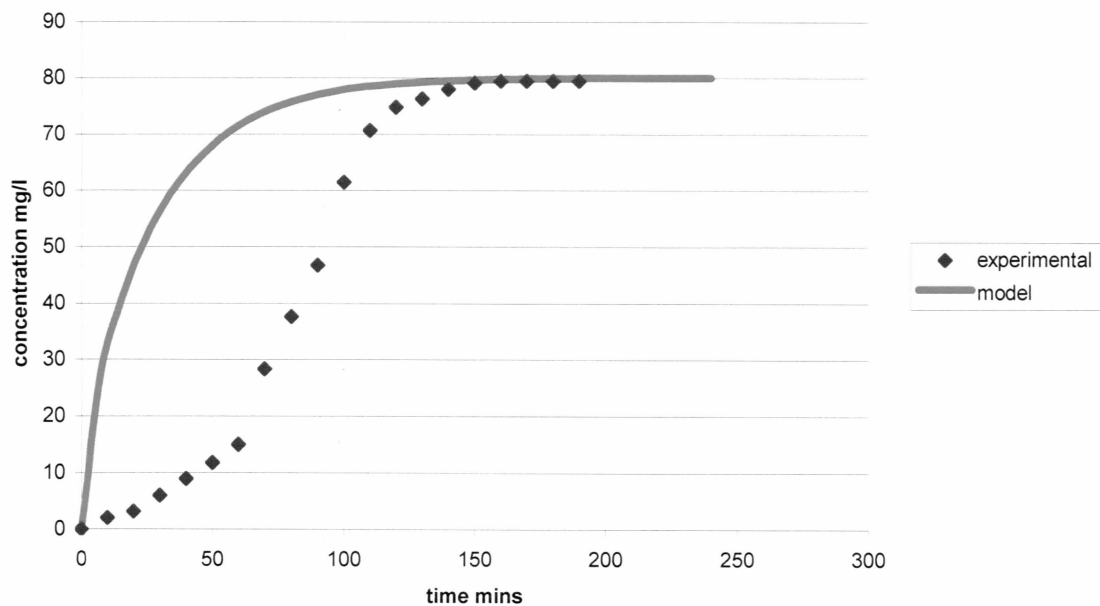


Figure 5.5. Comparison of numerical model results to elution test for sample 2.

The resulting minimum diffusion coefficient found from this test compares favorably with the results found from the source and receiving cells in the

through diffusion test. This favorable comparison gives a certain amount of credence to the assumption that was made to obtain this value.

The Mean square error method was followed to find the minimum diffusion coefficient. The results are presented in table below.

Table5.1 Mean square error for Sample 2 for various  $D_e$  values

$D_e$ values $m^2/s$	Mean square error
$1.23 \times 10^{-9}$	30.12
$9 \times 10^{-10}$	28.65
$5 \times 10^{-10}$	20.80
$1 \times 10^{-10}$	23.76

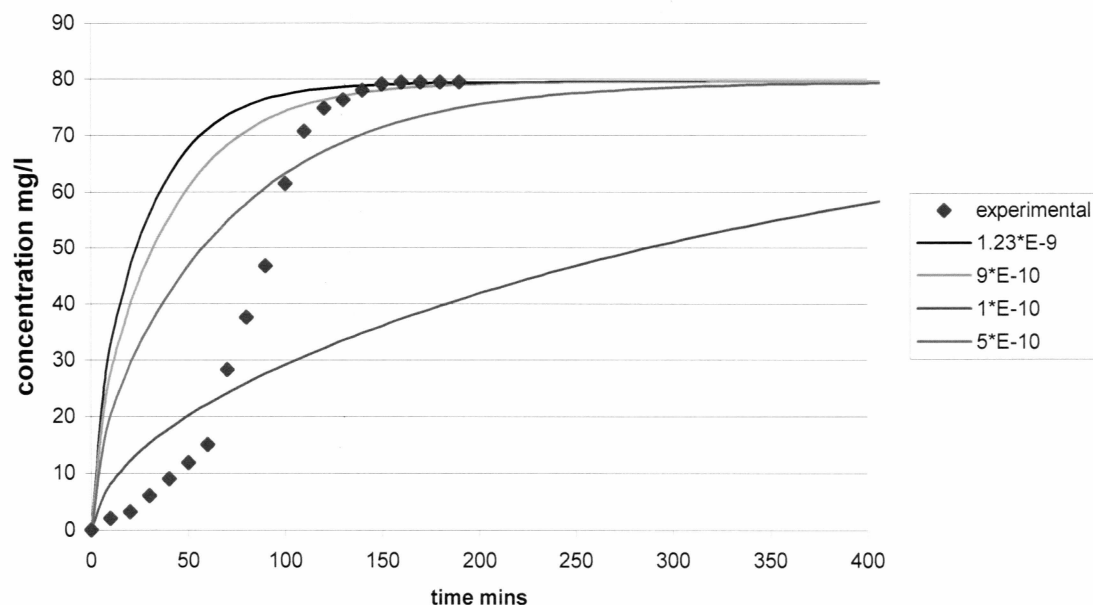


Figure 5.6 Comparison of numerical model to elution test of sample 2 for various  $D_e$  values.

The minimum value observed from the data is  $5 \times 10^{-11} \text{ m}^2/\text{s}$ , this value was not considered reliable because it over predicts the time necessary to reach the equilibrium. The experimental error due to lacking in stirring had probably lead to slower diffusion values in these experiments compared to experiments with stirring. The curve of  $5 \times 10^{-11} \text{ m}^2/\text{s}$  does not fit the later stages of experimental data. And hence minimum diffusion coefficient of  $1.23 \times 10^{-9} \text{ m}^2/\text{s}$  is considered

### 5.4 Sample 1 Elution Test

As discussed previously the through diffusion test for sample 1 was not successful. However, an indication of the diffusion coefficient can be obtained from comparing the numerical model results to the experimental data obtained for an elution test on sample A. Following the same assumption as discussed above with an additional assumption concerning the initial concentration of iodide in the rock pore space as was discussed in Section 4.5 the minimum effective diffusion coefficient was  $4 \times 10^{-11} \text{ m}^2/\text{s}$ . The comparison between the numerical model results and the experimental results are shown in Figure 5.7

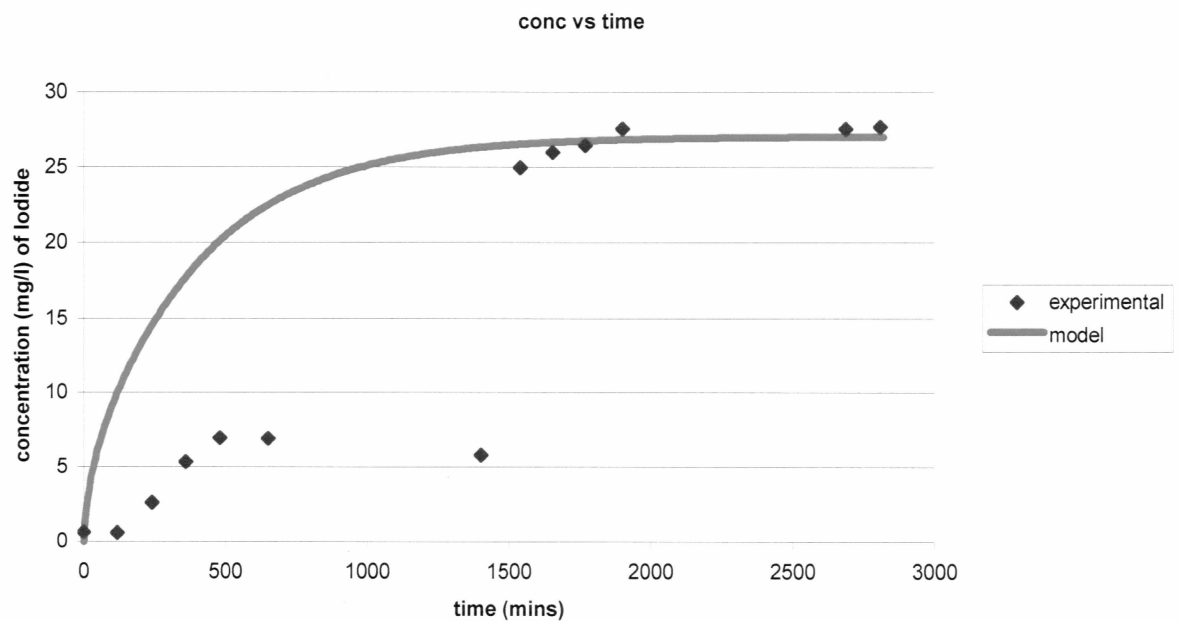


Figure 5.7. Comparison of numerical model results to elution test for sample 1.



The minimum effective diffusion coefficient obtained from this sample of the andesite core is two order of magnitude lower than the value obtained for sample 2. Examination of Figures 5.5 and 5.7 confirms this difference in values given the slow mass flux shown in Figure 5.7 in comparison to Figure 5.5. This result is noteworthy as it illustrates the spatial dependency of the effective diffusion coefficient.

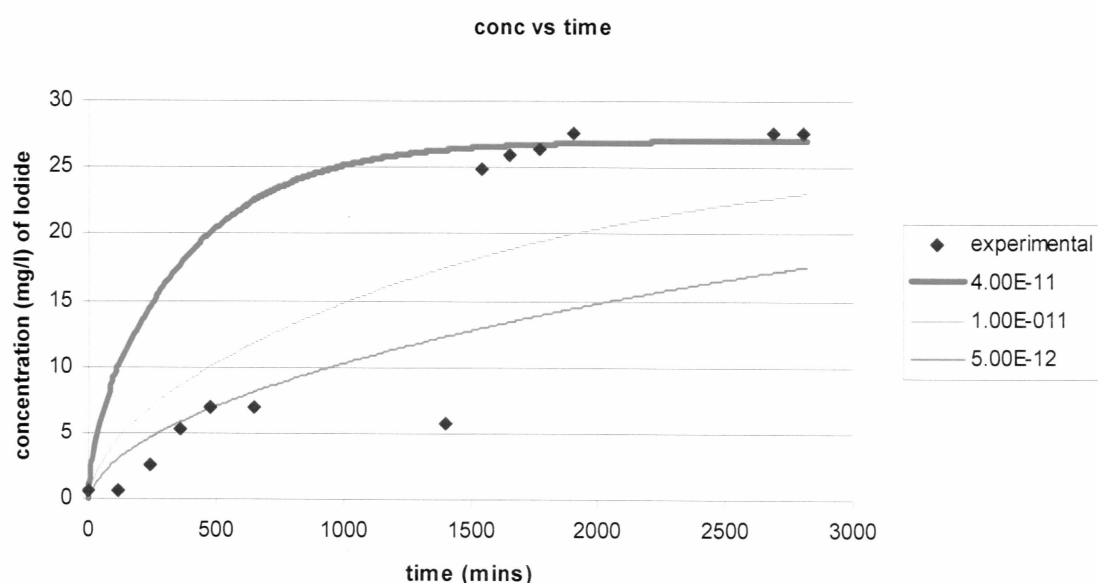


Figure 5.8 Comparison of numerical model to elution test of sample 1 for various  $D_e$  values.

The Mean square error method was followed to find the minimum diffusion coefficient. The results are presented in table below.

Table 5.2 Mean square error for Sample 1 for various  $D_e$  values

$D_e$ values	Mean square root
$4 \times 10^{-11}$	7.29
$5 \times 10^{-12}$	9.21
$1 \times 10^{-11}$	5.36

The minimum value observed from the data is  $1 \times 10^{-11} \text{ m}^2/\text{s}$ . But this value is not considered, as the curve obtained from the model should fit the data at the later stages of the experimental. The curve of  $1 \times 10^{-11} \text{ m}^2/\text{s}$  does not fit the later stages of experimental data. And hence minimum diffusion coefficient of  $4 \times 10^{-11} \text{ m}^2/\text{s}$  is considered.

A table summarizing the results from these two andesite samples is shown below.

Table 5.3 Effective diffusion coefficients of Andesite rock

Test	Effective diffusion coefficient ( $\text{m}^2/\text{s}$ )	
	Rock 1	Rock 2
Through diffusion (source cell)	-	$1.23 \times 10^{-9} \text{ m}^2/\text{s}$
Through diffusion (receiving cell)	-	$1.28 \times 10^{-9} \text{ m}^2/\text{s}$
Elution	$\geq 4 \times 10^{-11} \text{ m}^2/\text{s}$	$\geq 1.23 \times 10^{-9} \text{ m}^2/\text{s}$

There was a difference in effective diffusion coefficients ( $D_e$ ) because these  $D_e$  values are spread variably within the same rock type and through the rock mass.

As shown in the literature review in table 2.1 there were a range of effective diffusion coefficients ( $D_e$ ) values of different rock types. It was observed that the observed results were in the same magnitude as from the literature review.

### **5.5 Spatial Dependency of Effective Diffusion Coefficient**

As in sample 2, a formation factor can be calculated for sample 1, which results in a value of approximately 0.02, much less than the value for sample B. Isolating the ratio of constrictivity to tortuosity squared in Equation (7), results in a value of 0.42 for sample A and 4.96 for sample B. Given the relatively closer comparison between the ratios for these two samples in comparison to the effective diffusion coefficients, one can conclude that the majority of difference between the diffusive mass flux of iodide in these samples was the difference in porosity between these two rock samples.

As shown in the picture below we can observe a line across the andesite rock core. We do not know exactly whether it was a fracture or not. A simple test was done. The rock slice was placed in the slider of the reactor and one side of the reactor was filled with water and the other side was filled with little water and the reactor was made airtight to avoid evaporation. We found that there is no advection along the line. If this was assumed as a fracture then that could be the area of high porosity and this results in high mass flux rate.

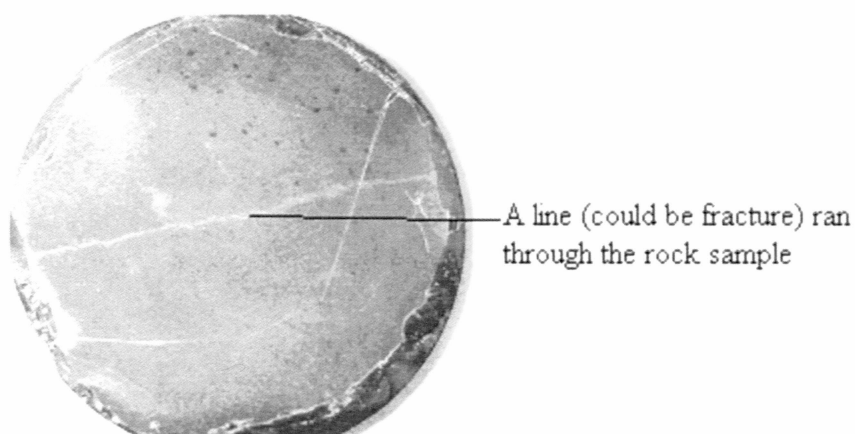


Figure.5.9 Picture of rock sample 2

From the picture taken while drying of the rock shown below, which were at time intervals of 45 seconds we can observe the drying patterns on the rock. This indicates the heterogeneity of the pore space.

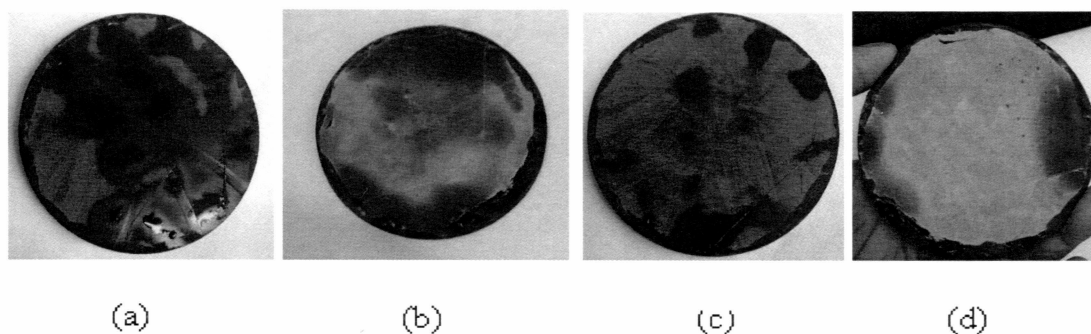


Figure 5.10. Drying of the rock from (a) to (d)

Diffusion has an influence in the movement of the radionuclides through the subsurface anthracite rocks found in Amchitka Island. When the radionuclides were flowing along with the water through the subsurface fractures then these radionuclides

tend to diffuse into the surrounding rock mass due to the concentration differences. There was an increase in the concentration of radionuclides in the rock mass. After a period of time when the concentration of radionuclides in the rock matrix was more than the concentration of radionuclides in the fracture then there is reverse diffusion of radionuclides from the rock matrix into the fracture. The radionuclides are then discharged into the seawaters.

A monitoring program needs to be taking into account the possible diffusion of radionuclides into the rock. The monitoring programs should focus at the bottom of the seabed and observe the radionuclides coming out from the island subsurface. If there is no diffusion taking place then the input of mass increases in a short period of time and hence a high peak will be seen. If there was diffusion into the rocks the input of mass would be same but was distributed or spread over a period of time.

## CHAPTER 6

### CONCLUSION

The purpose of this study was to better understand the movement of the radionuclides through Amchitka Island subsurface into the marine environment such that a monitoring program can be developed. Specifically, this research determined the effective diffusion coefficients for andesite rock obtained from the Island. The possibility of the radionuclide diffusion into the matrix rock surrounding the fractured pathways needs to be understood for a successful monitoring program.

Four tests were conducted; two through diffusion tests and two elution tests on two samples of andesite rock. The model was run changing two parameters; effective diffusion coefficient and porosity to match the experimental data obtained from the tests conducted. The model fit on to the experimental data was excellent for through diffusion test, but small deviations in experimental results of elution test versus model results were due to sorption of iodide onto the reactor materials.

Two rock slices obtained from the andesite rock core were used for measuring the effective diffusion coefficients. From the first elution test the effective diffusion coefficient observed was as low as  $4 \times 10^{-11} \text{ m}^2/\text{s}$  and porosity was 0.047. The effective diffusion coefficient of andesite rock in the successful through diffusion test was  $1.2 \times 10^{-9} \text{ m}^2/\text{s}$  and porosity was 0.041. The effective diffusion coefficient of second

andesite rock sample from elution test is  $1.2 \times 10^{-9} \text{ m}^2/\text{s}$  and porosity was observed as 0.153.

There was a difference in magnitude of effective diffusion coefficients when comparing both andesite rock samples. Others have shown that the effective diffusion coefficients are spatially variable within any specific rock type. Possible difference in porosities determined for the two different rock slices most likely contribute to the differences in the effective diffusion coefficients. After conducting these experiments it was observed that diffusion has an influence in the movement of the radionuclides through the subsurface anthracite rocks found in Amchitka Island.

**Recommendations for future research:**

This study was focused specifically on andesite rock. There are many rock types found on Amchitka Island: possible future studies can evaluate diffusion on other rock types to provide a more complete understanding of diffusion on Amchitka. This study is done on a piece of andesite rock sample that has a thickness of 3mm – 4.5mm. A study has to be done on a larger rock sample to observe the diffusion pathways. If possible it will be a good study how the diffusion rate in the rock mass near a fracture and rock mass away from the fracture. Run the same test again with different counter ion solution in the receiving cell to avoid advection.



## REFERENCES

- 1) Dubley, W.W., Balance, W.C. and V. M. Glanzman. "Hydrology." in The Environment of Amchitka Island, Alaska. (Edited by M.L.Meritt, et al.). Springfield, VA: Technical Information center, Environmental Research and Development Administration. (1977): 35-52.
- 2) Gard, L.M. "Geologic History." in The Environment of Amchitka Island. (Edited by M.L.Meritte, et al.). Springfield, VA: Technical Information center, Environmental Research and Development Administration. (1977): 13-34.
- 3) Everette, K.R. "Geomorphology." in The Environment of Amchitka Island. (Edited by M.L.Meritte, et al.). Springfield, VA: Technical Information center, Environmental Research and Development Administration. (1977): 161-178.
- 4) Merrit, M.L. "Geographic Setting." in The Environment of Amchitka Island. (Edited by M.L.Meritte, et al.). Springfield, VA: Technical Information center, Environmental Research and Development Administration. (1977): 1-12.
- 5) Powers, H. A., Coats, R.R., W.H.Nelson. "Geology and Submarine Physiography of Amchitka Island, Alaska." U.S Geological Survey Bulletin 1028-P. pp521-554.
- 6) Carr, W.J., W.D.Quinlivan, and L.M. Gard, 1970, Age and Stratigraphic Relations of Amchitka Island, Banjo point and Chitka point Formation, Amchitka Island, Alaska, in changes in Stratigraphic Nomenclature by the U.S. Geological Survey, 1969, G.V.Coh.G.Bates and W.B.Wright (Eds), pp. A16-A22, U.S.Geological Survey, Bulletin No.1324-A.

- 7) Gard L.M and B.J. Szabo, 1971, Age of the Pleistocene Deposits at Amchitka Islands, Alaska, Geol. Soc.Amer.,Abstr.with programs, 3(7):577
- 8) Gard L.M.,Jr.,G.E. Lewis, and F.C.Whitmore, Jr.,1972, Steller's Sea Cow in Pleistocene interglacial Beach Deposits on Amchitka, Aleutian Islands, Geol.Soc.Amer.,Bull.,83(3): 867-870.
- 9) Gates. Olcott, G.D.Fraser, and G.L.Snyder, 1954, Preliminary Report on the Geology of the Aleutian Islands, Science, 119(3092): 446-447.
- 10) Armstrong. R.H., "Air resources Laboratory-Las Vegas, National Oceanic and Atmospheric Administration, U.S. Department of Commerce, Las Vegas, Nevada." in The Environment of Amchitka Island. (Edited by M.L.Meritte, et al.). Springfield, VA: Technical Information center, Environmental Research and Development Administration. (1977): 53-58.
- 11) Fuller. R.G., J.B. Kirkwood "Ecological Consequences of Nuclear Testing" in The Environment of Amchitka Island. (Edited by M.L.Meritte, et al.). Springfield, VA: Technical Information center, Environmental Research and Development Administration. (1977): 627-649.
- 12) Fuller. R.G., 1971, Amchitka Bioenvironmental program. Amchitka Biological Information Summary, USAEC report BMI-171-132, Battelle Memorial Institute.
- 13) Kirkwood, J.B.(comp.), 1975, Bioenvironmental and Hydrologic Studies, Amchitka Island, Alasaka, Fall, 1974 Task Force Report, ERDA Report BMI-171-158, Battelle Memorial Institute.

- 14) Skagius K., and I. Neretneiks, Porosities and Diffusivities of some Nonsorbing Species in Crystalline Rocks. *Water Resources Research*, Vol 22, NO.3 pp 389-398, March 1986.
- 15) Feenstra. S, J.A. Cherry, E.A.Sudicky and Zia Haq, "Matrix diffusion effects on contaminant migratin from an injection well in fractured sand stone" *Ground water* Volume 22 No3, 1984: pp 307-316.
- 16) Nicole Ann Brown,"Modeling the diffusion of reactive and non reactive solutes in cores from Cannikin test site, Amchitka Island, Alaska". University of Nevada. Las Vegas. December 2000.
- 17) Tsukamoto. M and T. Ohe, Intra particle diffusion of cesium and strontium cation into rock materials. *Chemical geology*, 90(1991) 31-44.
- 18) Skagius K., and I. Neretneiks, Measurement of Cesium and Strontium Diffusion in Biotite Gneiss. *Water resources research*, vol.24, NO1, pp 75-84. January 1988.
- 19) Knox, R.C.,Sabatini,D.A. and L.W. Canter. *Subsurface Transport and Fate Processes*. Boca Raton, FL: Lewis Publishers. (1993): pp430.
- 20) Bradbury, M.H., and A. Green, Measurent of important Parameters determining aqueous phase diffusion rates through crystalline rock matrices. *Journal of hydrology*, 82 (1985): pp 39-55.
- 21) Foster, S.S.D. 1975, The chalk ground water tritium anomaly- a possible explanation. *Journal of hydrology*. V 25, pp 159-165.

- 22) Heath, M.J., M.Montoto, A. Rodriguez Rey, V.G. Ruiz de Argandona and B. Menendez, Rock matrix diffusion as a mechanism of radionuclide retardation: A natural analogue study of El Berrocal Granite, Spain.
- 23) Witthuser, K., B. Reichert, and H. Hotzl, Contaminant transport in fractured chalk: Laboratory and field experiments. Ground water, vol. 41, NO 6, 2003: pp 806-815
- 24) Long-Term Hydrological Monitoring Program: Amchitka, Alaska 1997. EPA, June 1998. NO: EPA-402-R-98-002.
- 25) Morrie, R.H., L.M.Gard and R.P. Synder, 1972, Visual Geological Effects of Cannikin Event, seismol. Soc.Amer.Bull., 62(6): 1519-1526.
- 26) Gonzalez, D.D., and L.E. Wollitz, 1972, Hydrological Effects of Cannikin Event, seismol. Soc.Amer.Bull., 62(6): 1527-1542.
- 27) Jacob Bear, Chin-Fu Tsang, Ghislain De Marsily, 1993, Flow and Contaminant Transport in Fractured Rock. Academic Press, Inc., Harcourt Brace Jovanovich, Publishers, 1993

## APPENDIX A

**Calibration curve for first through diffusion test:**

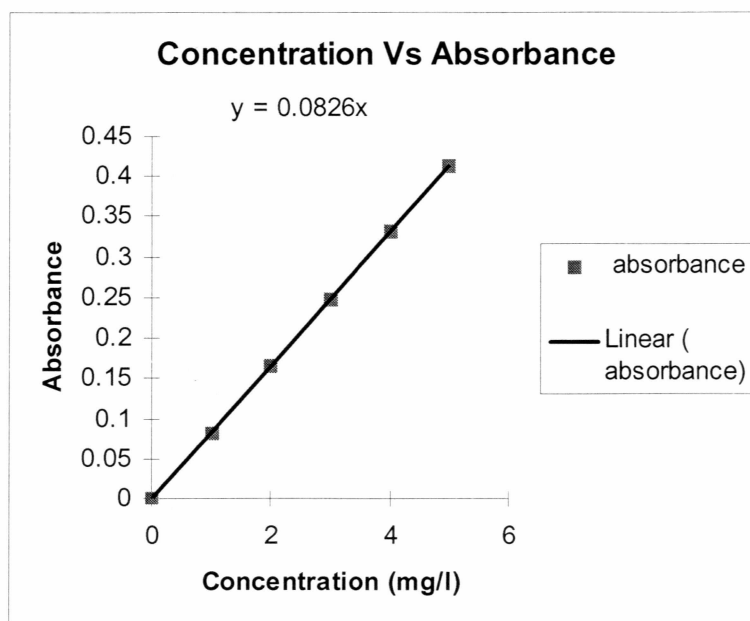


Figure A.1. Calibration curve for first through diffusion test.

**Experimental data for first through diffusion test:**

Table A.1 Experimental data for Through Diffusion test 1

Time(mins)	Ab a	Ab b	Ca (g/l)	Cb (g/l)
0			83	0
45	1.778	0.193	21.53038	2.337099
90	0.355	0.386	4.29881	4.674199
135	0.278	0.509	3.366392	6.163645
180	0.235	1.336	2.845691	16.17806
225	0.16	0.485	1.937492	5.873022
270	0.236	0.342	2.8578	4.141388
315	0.274	0.399	3.317954	4.83162
360	0.295	0.302	3.57225	3.657016
405	0.316	0.859	3.826546	10.40191
450	0.518	0.3	6.272629	3.632797
495	0.285	0.263	3.451157	3.184752

540	0.155	0.418	1.876945	5.061697
585	0.175	0.342	2.119132	4.141388
630	0.303	0.293	3.669125	3.548032
675	0.305	0.285	3.693344	3.451157
720	0.315	0.34	3.814437	4.11717
765	0.292	0.345	3.535922	4.177716
810	0.277	0.365	3.354282	4.419903
855	0.266	0.38	3.22108	4.601543
900	0.229	0.338	2.773035	4.092951
1412	0.7	0.42	8.476526	5.085916
1457	0.083	0.307	1.005074	3.717562
1502	0.45	0.369	5.449195	4.46834
1547	0.364	0.812	4.407794	9.83277
1592	0.504	0.661	6.103099	8.004262
1637	0.498	0.385	6.030443	4.662089
1682	0.379	0.273	4.589433	3.305845
1727	0.51	0.449	6.175755	5.437086
1772	0.525	0.402	6.357395	4.867948
1817	0.776	0.358	9.396835	4.335138
1862	0.409	0.41	4.952713	4.964822
1907	0.223	0.23	2.700379	2.785144
1952	0.543	0.385	6.575362	4.662089
1997	0.408	0.264	4.940604	3.196861
2042	0.404	0.36	4.892166	4.359356
2087	0.38	0.413	4.601543	5.00115
2888	0.378	0.482	4.577324	5.836694
2898	0.529	0.398	6.405832	4.819511
2985	0.369	0.494	4.46834	5.982006
3028	0.603	1.063	7.301922	12.87221

Ab a = absorbance in cell A

Ab b = absorbance in cell B

C a = concentration in cell A

C b = concentration in cell B

### Experimental data for first elution test:

Table A.2 Experimental data for elution test 1

Time (min)	Absorbance				Dilution	concentration mg/l of I
	1	2	3	Avg		
0	0.058	0.049	0.049	0.052	1:2	0.62953995
120	0.054	0.054	0.042	0.05	1:2	0.60532688
240	0.222	0.22	0.205	0.215667	1:2	2.61097659
360	0.453	0.439	0.431	0.441	1:2	5.33898305
480	0.566	0.578	0.571	0.571667	1:2	6.92090395
650	0.575	0.565	0.573	0.571	1:2	6.91283293
1400	0.472	0.49	0.47	0.477333	1:2	5.77885391
1540	0.402	0.42	0.413	0.411667	1:10	24.9192897
1655	0.427	0.429	0.43	0.428667	1:10	25.9483454
1770	0.44	0.436	0.434	0.436667	1:10	26.4326069
1900	0.46	0.454	0.45	0.454667	1:10	27.5221953
2688	0.46	0.454	0.45	0.454667	1:10	27.5221953
2808	0.458	0.467	0.45	0.458333		27.6437475

### Calibration curve for second through diffusion test:

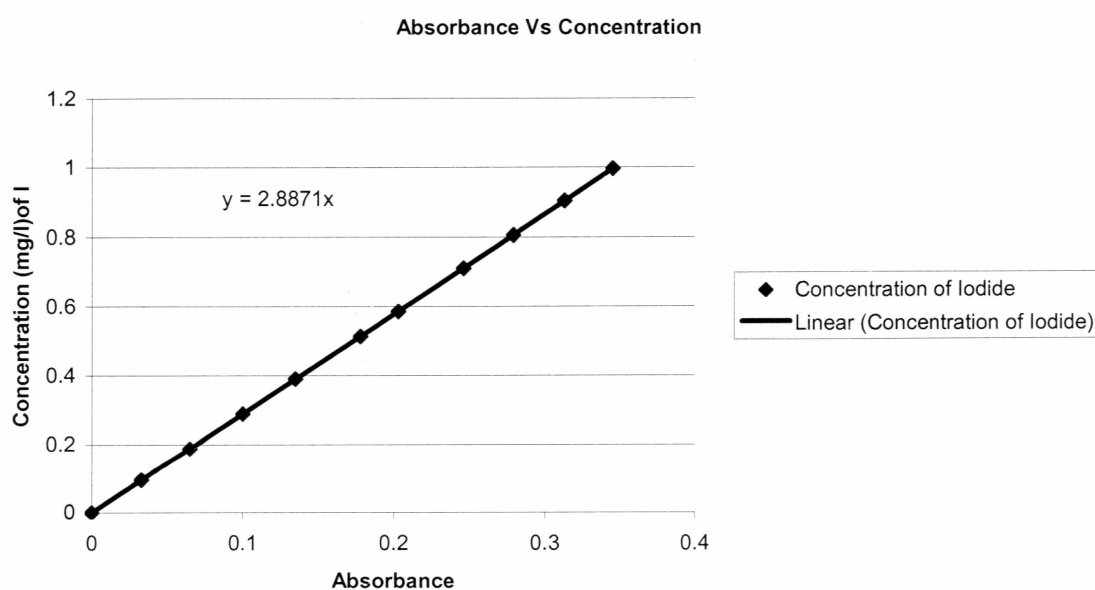


Figure A.2. Calibration curve for second through diffusion test.

### Experimental data from second through diffusion test:

Table A.3 Experimental data for Through Diffusion test 2

Time mins	absorbance A	absorbance B	concentration in	concentration in
			Cell A (mg/l) I	Cell B (mg/l) I
0	0.656	0	37.878752	0
45	0.582	0.073	33.605844	4.215166
75	0.444	0.196	25.637448	11.317432
105	0.338	0.308	19.516796	17.784536
150	0.232	0.389	13.396144	22.461638
195	0.309	0.321	17.842278	18.535182
240	0.324	0.301	18.708408	17.380342
285	0.329	0.297	18.997118	17.149374
330	0.319	0.307	18.419698	17.726794
375	0.305	0.322	17.61131	18.592924
420	0.319	0.298	18.419698	17.207116
465	0.313	0.312	18.073246	18.015504
510	0.312	0.314	18.015504	18.130988
555	0.316	0.312	18.246472	18.015504
600	0.313	0.313	18.073246	18.073246
645	0.315	0.312	18.18873	18.015504
690	0.315	0.313	18.18873	18.073246
735	0.313	0.313	18.073246	18.073246
780	0.312	0.313	18.015504	18.073246
825	0.312	0.312	18.015504	18.015504
870	0.316	0.31	18.246472	17.90002
915	0.314	0.312	18.130988	18.015504
960	0.318	0.314	18.361956	18.130988
1005	0.316	0.314	18.246472	18.130988



**Experimental data from second elution test:**

Table A.4 Experimental data for elution test 2

Time Mins	Absorbance	concentration mg/l
0	0	0
10	0.007	2.0209
20	0.011	3.1757
30	0.021	6.0627
40	0.031	8.9497
50	0.041	11.8367
60	0.052	15.0124
70	0.098	28.2926
80	0.13	37.531
90	0.162	46.7694
100	0.213	61.4931
110	0.245	70.7315
120	0.259	74.7733
130	0.264	76.2168
140	0.27	77.949
150	0.274	79.1038
160	0.275	79.3925
170	0.275	79.3925
180	0.275	79.3925
190	0.275	79.3925

## APPENDIX B

### Model program for through diffusion test:

REM Finite Difference solution for diffusion equation applied to the through  
REM diffusion experiment. Forward in time centered in space.

```
OPEN "d:\temp\cells.txt" FOR OUTPUT AS #1
OPEN "d:\temp\src.txt" FOR OUTPUT AS #2
OPEN "d:\temp\rec.txt" FOR OUTPUT AS #3
OPEN "d:\temp\mass.txt" FOR OUTPUT AS #4
```

```
DIM ncell(100)
DIM C$(100)
DIM Ct$(100)
```

REM Constants

REM -----

```
Co# = 37.8787      'Initial concentration (g/L)
De = .0000123#    'Effective diffusion coefficient (cm^2/s)
delt = .00025     'time step (hrs)
fint = 12.001     'final time (hrs)
delx = .01        'cell thickness (cm)
ncell = 45        'number of cells
r = 4.5           'radius of sample (cm)
por = .04         'rock porosity
srcV = 2.4        'source reservoir volume (L)
rcvV = 2.3        'receiving reservoir volume (L)
```

REM Unit conversion and constants

REM -----

```
delt = delt * 3600      'conversion of time step to seconds
fint = fint * 3600     'conversion of final time to seconds
B# = (De * delt) / (delx) ^ 2      'constant
porV# = 3.1415927# * (r ^ 2) * por * delx      'pore volume in one cell (cm^3)
Mo# = Co# * srcV        'initial mass of tracer in source reservoir (g)
Madd = 0!              'initial total mass contained in rock
```

REM Screen output

REM -----

```

CLS
PRINT "time="; 0; "hours"

REM Concentration calculation
REM -----
REM Initial conditions
  FOR i = 1 TO ncell + 1
    C#(i) = 0
  NEXT i

REM Time step calculation

10 FOR m = 1 TO fint / delt
  mrem# = 0
  t! = delt * m
  thr! = t! / 3600          'time in hours for output file

  tp! = 4 * thr! - FIX(4 * thr!)      'Define the time step to be printed
  IF tp! > .000015 GOTO 20
  PRINT "time="; thr!; "hours"

20 REM concentration at each time step
  FOR i = 1 TO ncell
    C#(0) = Co#                'initial concentration in source resevior (g/L)
    Ct#(ncell + 1) = Cres!
    Ct#(i) = B# * C#(i - 1) + (1 - (2 * B#)) * C#(i) + B# * C#(i + 1)
    mrem# = mrem# + (Ct#(i) * porV# / 1000)  'mass in rock
  NEXT i

  mrem# = mrem# + (Ct#(ncell + 1) * rcvV)    'mass remaining in source cell

REM cell concentration output
IF tp! > .000015 THEN GOTO 30
WRITE #3, Cres!
WRITE #1, Ct#(1), Ct#(2), Ct#(3), Ct#(4), Ct#(5), Ct#(6), Ct#(7), Ct#(8), Ct#(9),
Ct#(10), Ct#(11), Ct#(12), Ct#(13), Ct#(14), Ct#(15), Ct#(16), Ct#(17), Ct#(18), Ct#(19),
Ct#(20), Ct#(21), Ct#(22), Ct#(23), Ct#(24), Ct#(25), Ct#(26), Ct#(27), Ct#(28), Ct#(29),
Ct#(30), Ct#(31), Ct#(32), Ct#(33), Ct#(34), Ct#(35), Ct#(36), Ct#(37), Ct#(38), Ct#(39),
Ct#(40), Ct#(41), Ct#(42), Ct#(43), Ct#(44), Ct#(45)

```

```

30 REM relabel concentrations for next time step
  FOR i = 1 TO ncell + 1
    C#(i) = Ct#(i)
  NEXT i

REM New concentration in source and receiving cells (g/L)
Co# = (Mo# - mrem#) / srcV          'source cell
IF tp! > .000015 GOTO 40            'output
  WRITE #2, thr!, Co#
40 Cres! = C#(ncell)                'receiving cell

REM Total Mass Balance
Mrock = 0
FOR i = 1 TO ncell
  Mrock = C#(i) * porV# / 1000 + Mrock
NEXT i
Mtot# = Mrock + Co# * srcV + Cres! * rcvV

IF tp! > .000015 GOTO 50            'mass balance output
WRITE #4, thr!, Mtot#

50 NEXT m

CLOSE #1, #2, #3, #4

```

### Model program for elution test:

REM Finite Difference solution for diffusion equation applied to the out  
 REM diffusion experiment. Forward in time centered in space.

```

OPEN "d:\temp\cells.txt" FOR OUTPUT AS #1
OPEN "d:\temp\rec.txt" FOR OUTPUT AS #2
OPEN "d:\temp\mass.txt" FOR OUTPUT AS #3

```

```

DIM ncell(100)
DIM C#(100)
DIM Ct#(100)

```

REM Constants

REM -----

Co# = 23.1        'Initial concentration (g/L)  
 De = .00000009#    'Effective diffusion coefficient (cm<sup>2</sup>/s)  
 delt = .00025      'time step (hrs)  
 fint = 47.001      'final time (hrs)  
 delx = .01        'cell thickness (cm)  
 ncell = 45        'number of cells  
 r = 4.5           'radius of sample (cm)  
 por = .07          'rock porosity  
 rcvV = 1!          'receiving reservoir volume (L)  
 delta = .0015

delt = delt \* 3600            'conversion of time step to seconds  
 fint = fint \* 3600           'conversion of final time to seconds  
 B# = (De \* delt) / (delx) ^ 2        'constant  
 porV# = 3.1415927# \* (r ^ 2) \* por \* delx    'pore volume in one cell (cm<sup>3</sup>)  
 Mo# = Co# \* porV# \* ncell / 1000            'initial mass of tracer in source reservoir (g)

CLS

PRINT "time ="; 0; "hours"

REM concentration calculation

REM -----

REM Initial conditions

IF t > 0 GOTO 10  
 FOR i = 1 TO ncell  
 C#(i) = Co#  
 NEXT i

REM Time step calculation

10 FOR m = 1 TO fint / delt  
 mrem# = 0  
 t! = delt \* m  
 thr! = t! / 3600                    'time in hours for output file

```
tp! = 8 * thr! - FIX(8 * thr!)
```

```
IF tp! > delta GOTO 20
```

```
PRINT "time="; thr!; "hours"; tp!
```

```
20 REM concentration at each time step
```

```
FOR i = 1 TO ncell
```

```
Ct#(ncell + 1) = Crec!
```

```
Ct#(0) = Crec!
```

```
Ct#(i) = B# * C#(i - 1) + (1 - (2 * B#)) * C#(i) + B# * C#(i + 1)
```

```
mrem# = mrem# + (Ct#(i) * porV# / 1000)
```

```
NEXT i
```

```
IF tp! > delta THEN GOTO 30
```

```
WRITE #1, Ct#(1), Ct#(2), Ct#(3), Ct#(4), Ct#(5), Ct#(6), Ct#(7), Ct#(8), Ct#(9),  
Ct#(10), Ct#(11), Ct#(12), Ct#(13), Ct#(14), Ct#(15), Ct#(16), Ct#(17), Ct#(18), Ct#(19),  
Ct#(20), Ct#(21), Ct#(22), Ct#(23), Ct#(24), Ct#(25), Ct#(26), Ct#(27), Ct#(28), Ct#(29),  
Ct#(30), Ct#(31), Ct#(32), Ct#(33), Ct#(34), Ct#(35), Ct#(36), Ct#(37), Ct#(38), Ct#(39),  
Ct#(40), Ct#(41), Ct#(42), Ct#(43), Ct#(44), Ct#(45), Ct#(46), Ct#(47), Ct#(48), Ct#(49),  
Ct#(50)
```

```
30 FOR i = 1 TO ncell + 1 'relabel concentrations for next time step
```

```
C#(i) = Ct#(i)
```

```
NEXT i
```

```
REM Mass balance in rock
```

```
REM -----
```

```
Crec# = (Mo# - mrem#) / rcvV'new concentration of tracer in receiving resevoir (g/L)
```

```
IF tp! > delta GOTO 40
```

```
WRITE #2, thr! * 60, Crec# * 1000
```

```
40 REM Total Mass Balance
```

```
REM -----
```

```
Mrock = 0
```

```
FOR i = 1 TO ncell
```

```
Mrock = C#(i) * porV# / 1000 + Mrock
```

```
NEXT i
```

$M_{tot\#} = M_{rock} + C_{rec!} * rcvV$

IF  $tp! > \delta$  GOTO 50  
WRITE #3,  $thr!$ ,  $M_{tot\#}$

50 NEXT  $m$

CLOSE #1, #2, #3